Tissue Oxymetry Using Magnetic Resonance Spectroscopy

by

Lisa Chiawen Liu

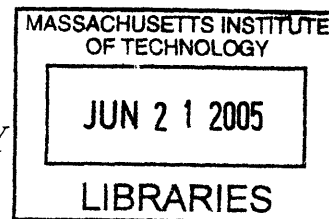B.A., Chemistry, Scripps College (2002)

Submitted to the Department of Chemistry
in partial fulfillment of the requirements for the degree of

Master of Science in Chemistry

at the

MASSACHUSETTS INSTITUTE OF TECHNOLOGY

June 2005
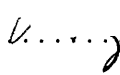
Author . . . .
Department of Chemistry
May 20, 2005
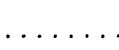
Certified by . . . .
Bruce Jenkins
Instructor in Radiology at Harvard Medical School
Thesis Supervisor

Certified by . . . .
A Gregory Sorensen
Associate Professor in Radiology at Harvard Medical School
Thesis Supervisor

Certified by . . . .
Moungi G. Bawendi
Professor of Chemistry
Thesis Supervisor

Accepted by . . . .
Robert W. Field
Chairman, Department Committee on Graduate Students

Tissue Oxymetry Using Magnetic Resonance Spectroscopy

by

Lisa Chiawen Liu

Submitted to the Department of Chemistry
on May 20, 2005, in partial fulfillment of the
requirements for the degree of
Master of Science in Chemistry

Abstract

A noninvasive method for in vivo measurement of tissue oxygen concentration has been developed. Several techniques currently used suffer limitations that prevent their practical clinical use. Our method is to use the paramagnetism of molecular oxygen to build a method for noninvasive tissue oxymetry. By using paramagnetism of molecular oxygen, magnetic resonance spectroscopy (MRS) can be used to measure tissue oxygenation. Chemical shifts of brain metabolites and water have a downfield shift with increased amounts of oxygen. Chemical shifts were linearly dependent on the fraction of inspired oxygen (FIO_2) and the slope is approximately 0.0003 ppm per percent change of oxygen. The slope was not significantly different between brain metabolites or water. Furthermore, the slope agreed with simple theoretical predictions using Henry's law and the magnetic susceptibility of molecular oxygen. Changes in brain oxygenation in the same animals was confirmed using gradient echo BOLD measurements of changes in R2* as a function of FIO_2 in the same animals. The results demonstrated the promising potential of this technique. The implementation of this method in stroke and tumor models is discussed.

Thesis Supervisor: Bruce Jenkins
Title: Instructor in Radiology at Harvard Medical School

Thesis Supervisor: A Gregory Sorensen
Title: Associate Professor in Radiology at Harvard Medical School

Thesis Supervisor: Moungi G. Bawendi
Title: Professor of Chemistry

Acknowledgments

Contents

List of Figures

10

Chapter 1

Introduction

The concentration of oxygen in tissue is a major parameter describing organ viability, and tissue oxygen content is a vital parameter for a number of important pathologies. Regional oxygen tension, which reflects the overall health of tissue, depends on the extent of perfusion and the level of local metabolic activity requiring oxygen consumption. Effective radiotherapy for tumors requires tissue to be well-oxygenated. Recently, hyperoxia has been found to reduce infarct size after stroke [26]. In addition, tissue oxygen saturation can change during activation associated with normal brain activity as well as in states such as status epilepticus, in which energy demands greatly increase [25] [24]. Many magnetic resonance (MR) techniques have been used for the measurement of oxygen tension, or parameters related to oxygenation. Unfortunately, there are no effective, non-invasive methodologies for accurate quantification of local tissue pO_2. While very safe and effective methodologies exist for measurement of arterial oxygen saturation, the methods that exist for non-invasive, in vivo measurement of tissues such as the brain are quite limited. We propose to perform experiments relevant to the development of more comprehensive MR measures of local tissue pO_2. The advantages and disadvantages of a number of MR techniques that have been used for measurement of local tissue oxygen content will be discussed in the following sections.

1.1 BOLD

The most common MR technique for obtaining oxygenation-dependent information is a semi-quantitative approach that relies upon the changes in magnetic field gradients around blood vessels due to changes in the oxygenation states of iron in hemoglobin. Structure of hemoglobin is shown in figure 1-1 which is taken from www.people.virginia.edu/rjh9u/hemoglob.html.
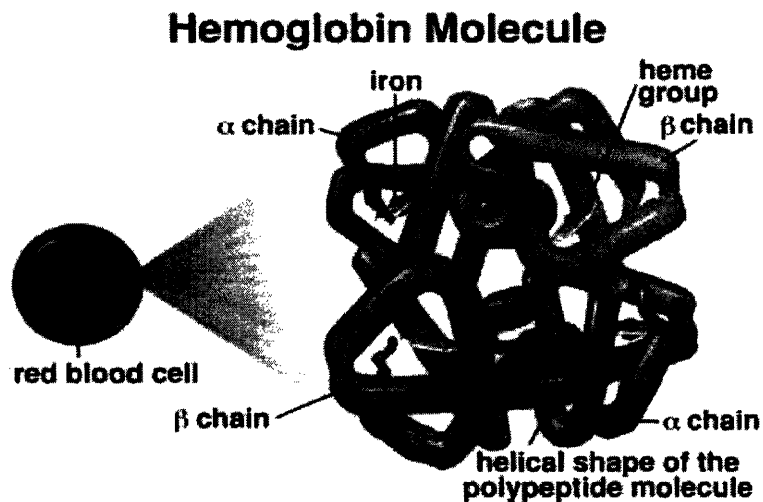
Figure 1-1: Structure of the hemoglobin.

This method is referred to as BOLD (blood oxygenation level dependent contrast) [21]. The origins of this technique go back to the 1930's with Pauling's work [23] which demonstrated changes in magnetic susceptibility of hemoglobin depending upon its oxygenation state. The figure 1-2 shows structural change of hemoglobin during the oxygen binding process. The picture is taken from www.chemistry.wustl.edu/-edudev/LabTutorials.

The spin state of the iron changes from 2 to 0 when O_2 binds reversibly to iron-porphyrin active sites in hemoglobin and causes deoxyhemoglobin to be paramagnetic. The paramagnetic nature of deoxyhemoglobin causes a local magnetic field inhomogeneity which can be exploited by MR techniques to obtain information about deoxyhemoglobin concentration and therefore oxygenation. However, the BOLD signal can

14
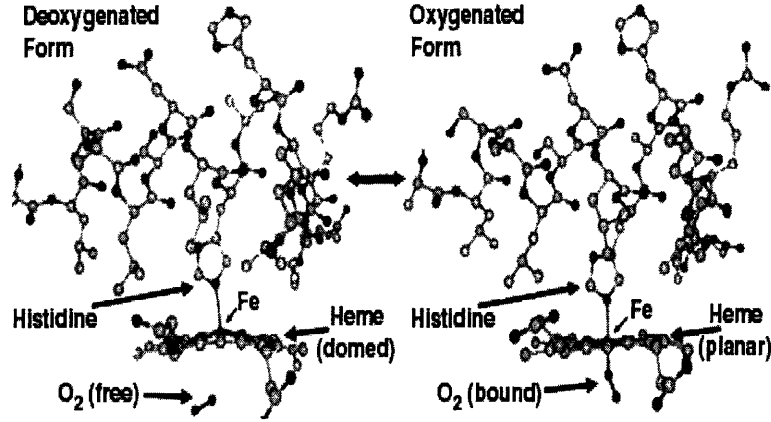
Figure 1-2: When hemoglobin is deoxygenated as shown at the left, the heme group adopts a domed configuration. When hemoglobin is oxygenated as shown at the right, the heme group adopts a planar configuration. The conformational change in the heme group causes the protein to change its conformation.

be affected by changes in blood flow, blood volume, motion, and anything else that leads to a change in T2*. T2* is the empirical constant associated with the decay of the transverse magnetization. The BOLD contrast is dependent upon blood flow and oxygen consumption as described below [10]:

$$\Delta R_2^* BOLD(t) \propto vf(t)\frac{CMRO_2(t)^{\beta}}{CBF(t)} - vf(0)\frac{CMRO_2(0)^{\beta}}{CBF(0)}, \tag{1.1}$$

where $\Delta R2^*$ ($=1/T2^*$) is the change in the transverse relaxation rate,$CMRO_2(t)$ is the oxygen consumption and $CBF(t)$ is the blood flow. Thus, extraction of oxygenation from measurements at a single oxygenation state is quite difficult. One recent paper examined the utility of BOLD for examining pO_2 in tumors by comparing BOLD measurements with measurements made from a regional implanted oxygen electrode. These data are shown in Figure 1-3 below
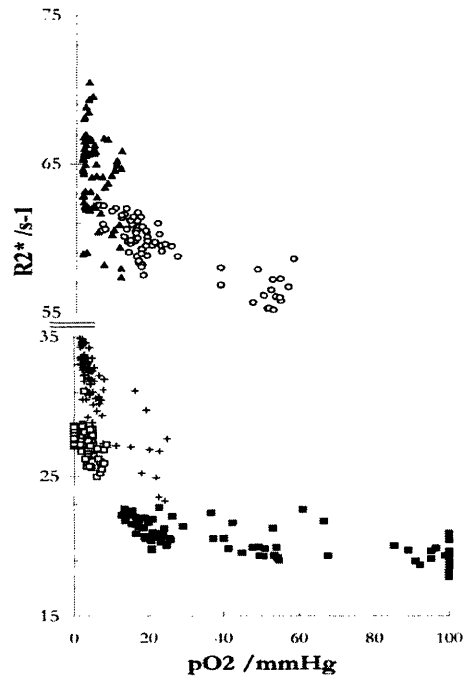
Figure 1-3: Variation in local R2* as a function of variations in pO_2. Each symbol represents a different tumor. Note that the sensitivity of R2* to changes in pO_2 is variable from one tumor to another. Note also that a given value of R2* is not predictive of the pO_2 value. This picture is taken from Figure 5 of [3].

16

While there was in general an excellent correlation between the measured pO_2 and the R2* value, it was determined that absolute quantification of pO_2 was impossible with BOLD [3] [4]. The reason for the failure of this technique is that it is impossible to turn an R2* value directly into a pO_2 value.

1.2 Measurement of T1

Another method is to measure the effect of oxygenation on the T1 (longitudinal relaxation time) [12]. In this approach the researchers investigated whether the O_2 dissolved during hyperoxygenation is responsible for the reduction of T1 rather than O_2 bound to hemoglobin. They found that there was a negative linear relationship between pO_2 and T1.
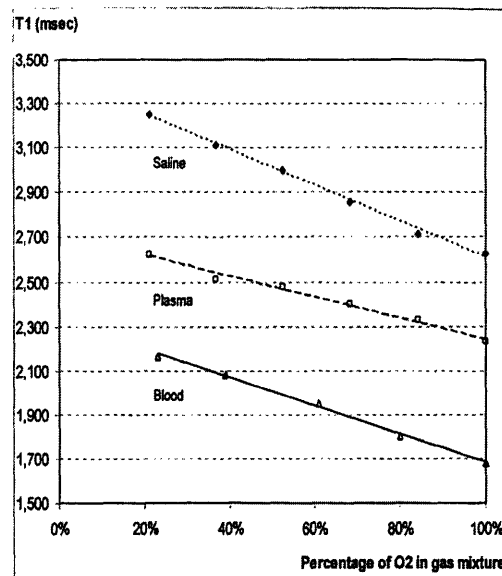
Figure 2. T1 in solutions saturated with varying gaseous O_2 concentrations (8.45-Tesla magnet).

Figure 1-4: Measurement of T1 with various oxygen percentage in three solutions. This image is taken from [12].

17

They believed that the dissolved molecular oxygen contributed to this reduction of T1 during hyperoxygenation. The authors claimed that during hyperoxygenation, the free fraction of O_2 that is dissolved in the solution is the main source of the reduction of T1 due to its paramagnetic properties. However, like T2* signals, T1 signals are complex and many biological factors can lead to a change of T1 signal, including, importantly, changes in blood flow. Furthermore, measurements during hyperoxia may not be relevant to the normal physiologic state. Thus, it is not possible to measure pO_2 quantitatively by change of T1 signals alone.

1.3 ^{19}F Spectroscopy and Imaging

In another technique, the linear dependence of the T1 relaxation rate of perfluorinated contrast medium (PFC) on oxygen content is used. It was found that the longitudinal relaxation rate (1/T1=R1) of the fluorine nucleus depended linearly on the partial pressure of oxygen. For this approach, PFC has to be delivered to the tissue being sampled, and fluorine 19 MR imaging is used to measure R1 [1]. The researchers used perfluorotributylamine to investigate the relationship between the longitudinal relaxation rate of the fluorine nucleus and partial pressure of oxygen [22]. The data from this study is shown in Figure 1-5 taken from http://cip.swmed.edu/LPR/pO_2.htm.
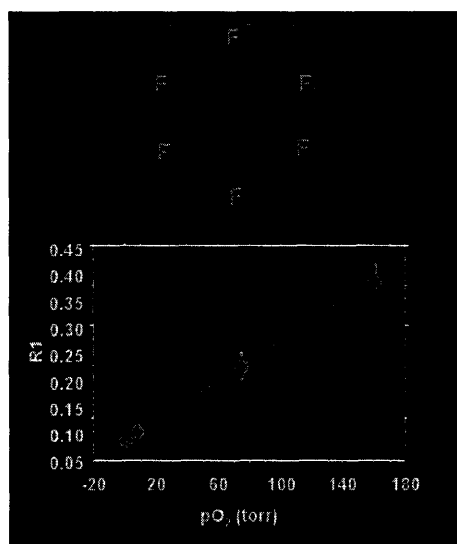
Figure 1-5: The longitudinal relaxation rate of fluorine nucleus linearly increased with pO_2 [1]

pO_2 maps are then produced from calculated ^{19}F T1 images of PFCs through application of the calibration curve data from the linear relationship between PFC ^{19}F relaxation rate and pO_2 [9] [20]. The major limitation of this technique is the low signal to noise ratio (SNR) of $^{(19)F}$ NMR and the requirement injection of an exogenous agent. These limitations make this approach impractical for routine human use.

1.4 ^{17}O Methods

Another MR spectroscopic method is measurement of ^{17}O MR signal after inhalation of gaseous ^{17}O. Detection of ^{17}O may be done directly by ^{17}O MR imaging or spectroscopy, or indirectly by detecting the effect of ^{17}O on a ^1H water image [32] [31] [29].
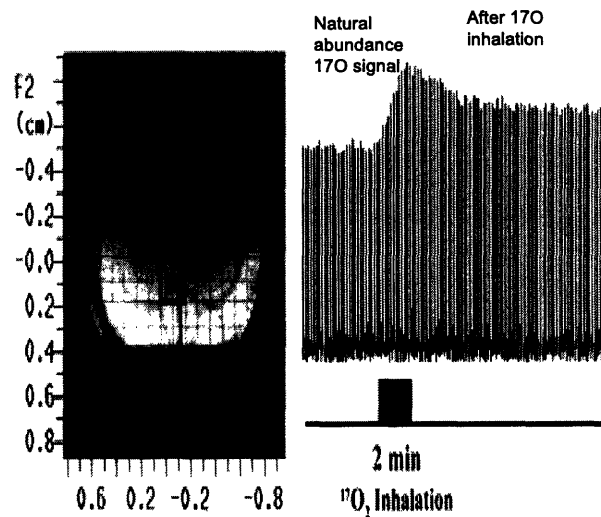
Figure 1-6: ^{17}O signals increased after breathing ^{17}O label oxygen for two minutes. This illustration is taken from [32]

The direct method suffers from poor sensitivity and hence poor spatial resolution. Some researchers have tried to solve the sensitivity problem through ultra high-field ^{17}O chemical shift imaging, which shows a fourfold increase in NMR sensitivity from 4.7T to 9.4T and can rapidly image the $CMRO_2$ (cerebral metabolic rate of oxygen consumption) in the rat. The experiment demonstrated several advantages; however, the procedure required an invasive implantation of a ^{17}O radiofrequency receiver coil that would not be applicable to humans. Furthermore, ^{17}O is quite expensive and requires injection in the subject, and there are problems involved in modeling the H_2O formation in brain due to the influx of labeled water from large metabolically active tissues such as the liver. Again, this approach has not found wide acceptance.

1.5 EPR

Finally, EPR (electron paramagnetic resonance) methods including both spectroscopic and imaging systems are used to generate possible oxygen quantification methods. A major problem with EPR imaging is the heating of the imaged object due to the dielectric loss during the imaging process. This restricts its use to only small tissue samples or small animals. Researchers were able to solve this problem by using the Overhauser effect to indirectly detect the EPR-signal [13] with a new contrast medium based on a single electron substance [16] [15] to enhance the signal through dipole-dipole interaction. This signal enhancement is a function of RF power and of the EPR linewidth of the substance, which is influenced by the oxygen concentration. However, the downside of the Overhauser EPR is the requirement of special equipment such as the special low magnetic field scanner.
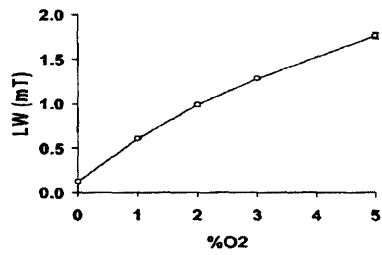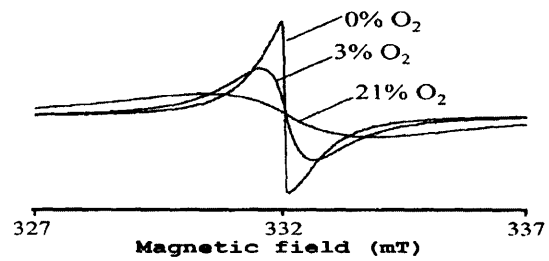
FIG. 1. Sensitivity of the EPR linewidth to the oxygen environment.
Results obtained using Printex U. Top: EPR spectra recorded in
X-Band (9 GHz) in different oxygen environments. Bottom: Calibra-
tion curve of the Printex U in a muscle homogenate.

Figure 1-7: The linewidth is increasing with percentage of oxygen. The image is taken from [17].

Carbon blacks [17] were demonstrated to be suitable EPR contrast media and they have several advantages such as long-term stability and absence of toxicity. However, we would like to find an endogenous way to measure pO_2 without injecting or using any contrast medium in the human body. Also, another crucial disadvantage of this method is the power deposition caused by the EPR B1 field, which might cause undesired heating, especially above 300 MHz.

In summary, while a variety of approaches have shown sensitivity to tissue pO_2, none have shown the ability to absolutely quantify pO_2 levels non-invasively.

1.6   Motivation and Rationale

After reviewing several commonly-used MR techniques for measuring tissue oxygenation, we are motivated to develop a technique that will avoid some of the limitations outlined above. First, we want to use a paramagnetic endogenous contrast agent such as molecular oxygen that requires no injection or implantation and can be exploited by MR techniques. Second, by using ^1H MR, we solve the low sensitivity problems that ^{19}F and ^{17}O encountered. Thus, we hypothesize that magnetic resonance spectroscopy can be used to measure the chemical shifts of brain metabolites and water that are induced by paramagnetic molecular oxygen and we can explicitly demonstrate the relationship between chemical shift and molecular oxygen.

1.7   Thesis overview

Chapter 2 will describe the theory behind our proposed technique. Chapter 3 will contain a detailed description of our experimental procedure. Chapter 4 will present the results that we obtained from our proposed technique. Chapter 5 will contain the summary and outline the future work on our technique and possible implementation of this technique in clinical practice.

Chapter 2

Theory

2.1 Introduction

In this section, the advantage of paramagnetism as an essential property to use in measuring tissue oxygenation will be discussed. Also, how paramagnetism will affect the chemical shift and how relaxivity is influenced by paramagnetism will be discussed.

2.2 Paramagnetism and chemical shift

2.2.1 Paramagnetism

A paramagnetic material is one whose atoms have permanent dipole moments. If a magnetic field is applied to such a material, the dipole moments try to line up with the magnetic field, but are prevented from becoming perfectly aligned by their random thermal motion. Because the dipoles try to line up with the applied field, the susceptibilities of such materials are positive, but in the absence of a strong ferromagnetic effect, the susceptibilities are rather small, say in the range 10^{-5} to 10^{-3}.

If, on the average, only a relatively small fraction of the atoms are aligned with the field, then the magnetization obeys Curie's law:

$$M = C\frac{B_{ext}}{T} \tag{2.1}$$

where C is a constant (different for each different material), where T is the temperature in Kelvins, and where B_{ext} is the applied magnetic field. Curie's law says that if B_{ext} is increased, the magnetization increases (the stronger magnetic field aligns more of the dipoles). It also says that if the temperature is increased, the magnetization decreases (the increased thermal agitation helps prevent alignment). Curie's law only works for samples in which a relatively small fraction of the atoms are aligned, on the average, with the magnetic field.

When a paramagnetic material is placed in a strong magnetic field, it reinforces the applied field, and as long as the strong magnetic field is present, it will remain magnetized. But when the strong magnetic field is removed, the net magnetic alignment is lost as the dipoles relax back to their normal random motion.

The ground-state electron configuration of O_2 is

$$KK(\sigma 2_s)^2(\sigma * 2_s)^2(\pi 2p_x)^2(\pi 2p_y)^2(\sigma 2p_z)^2(\pi * 2p_x)^1(\pi * 2p_y)^1 \tag{2.2}$$

According to Hund's rule, the $\pi * 2p_x$ and $\pi * 2p_y$ orbitals are occupied by one electron such that the spins of the electrons are parallel. Therefore, an oxygen molecule has a net electron spin and is paramagnetic. This means that oxygen is attracted to a region between the poles of a magnet. A particularly interesting demonstration of this is shown in Figure 2-1 which is taken from http://demoroom.physics.ncsu.edu/.
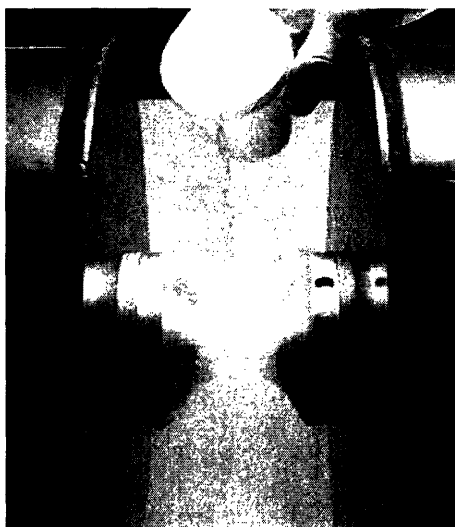
Figure 2-1: An oxygen molecule in its ground electron state has two unpaired electrons, and so has a net electronic spin. This net spin causes an oxygen molecule to act as a tiny magnet. Therefore, oxygen is a magnetic substance and is attracted to a region between the poles of a magnet as shown above.

Magnetic field produced
by circulating electron
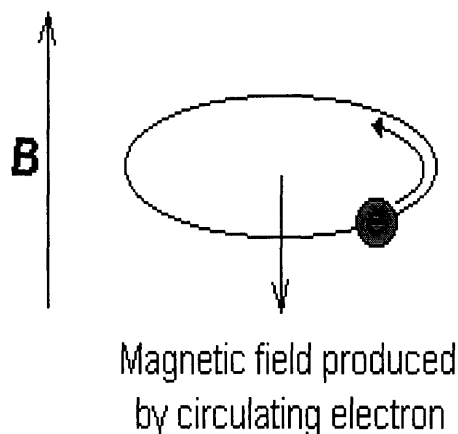
Figure 2-2: The magnetic field at the nucleus is not equal to the applied magnetic field; electrons around the nucleus shield it from the applied field.

2.2.2 Chemical shift

The magnetic field at the nucleus is not equal to the applied magnetic field. The electrons around the nucleus shield it from the applied field. The difference between the applied magnetic field and the field at the nucleus is called nuclear shielding or chemical shift. Chemical shift is a function of the nucleus and its environment. The demonstration 2-2 is taken from www.shu.ac.uk/schools/sci/chem/tutorials/molspec/nmr1.

The chemical shift can be influenced by many factors including: the diamagnetic contribution, the paramagnetic contribution, the neighbor anisotropy effect, the ring-current contribution, the electric field effect and the solvent effect. We are interested in the paramagnetic effect on the chemical shift.

Paramagnetic compounds have unpaired electrons and their magnetic susceptibility, χ, is positive. Interactions between paramagnetic centers and other molecules can lead to what are know as Fermi contact interactions between the nuclear spin and the unpaired electron. These interactions lead to alterations in the chemical shifts of the nuclear spins. Years ago, before the onset of high static magnetic fields this effect was used to generate large shifts that enabled separation of overlapping protons. Such paramagnetic agents were known as shift reagents.

We are interested in the paramagnetic effect on the chemical shift [19] [11] [7].

28

An addition of paramagnetic species will shift the nuclear resonances. In the NMR spectrum of a paramagnetic species, the total observed chemical shift is described by

$$\delta_{obs} = \delta_{dia} + \delta_{pm} \tag{2.3}$$

where δ_{obs} is observed, δ_{dia} is diamagnetic, and δ_{pm} is paramagnetic shift. The paramagnetic shift can be expressed as sum of three different contributions [28],

$$\delta_{pm} = \delta_{con} + \delta_{dip} + \delta_{\chi} \tag{2.4}$$

where δ_{con} is the complex formation shift, δ_{dip} is the dipolar contribution, and δ_{χ} is the bulk magnetic susceptibility (BMS) shift. The two former mechanisms are known as the hyperfine interaction. The hyperfine interaction requires at least transient chemical bonding between the nondiamagnetic agent molecule and the host molecule bearing the nuclear spin of interest. The BMS interaction specifically does not involve such bonding. Another important distinction between complex formation shift and the bulk magnetic susceptibility shift is that the hyperfine shift is quite specific for each kind of nuclear spin, whereas the BMS shift is the same for any nuclear spin in a given location in any particular compartment. If we are interested in measuring shifts due to dissolved oxygen, the likelihood that direct interactions between O_2 and water (or other molecules) will lead to any hyperfine interaction shifts is small. More likely, the O_2 will lead to a change in bulk magnetic susceptibility. The δ_{χ}, the BMS shift, can be expressed as in

$$\Delta\chi = \delta_{\chi} - \delta_{\chi}(0) \tag{2.5}$$

where δ_{χ} is the BMS contribution to the frequency of spins when an agent is present and $\delta_{\chi}(0)$ is the contribution when all other terms are the same and only the agent is absent. We can thus express the BMS effect from oxygen as

$$\Delta\chi = [O_2]\chi_{O2} \tag{2.6}$$

29

where $[O_2]$ is the concentration of the oxygen in the tissue and χ_{O2} magnetic susceptibility of the oxygen. Therefore, we can predict $\Delta\chi$ from magnetic susceptibility of the oxygen and by using Henry's constant of the oxygen or solubility coefficient of oxygen in the blood, we can relate partial pressure of oxygen (pO_2) to concentration of oxygen in the tissue. Mass magnetic susceptibility of the oxygen is $133.6 * 10^{-8}$ m^3/Kg and the Henry's Law constant of oxygen at 37 Celsius is around $1.04 * 10^{-2}$ mol/L-atm. By doing some calculations for unit conversion,

$$133.6\text{x}10^{-8}\tfrac{m^3}{kg} \times 1.04 \times 10^{-2}\tfrac{mole}{L-atm} \times \tfrac{0.00132atm}{mmHg} \times \tfrac{32g}{mole} \times \tfrac{1kg}{1000g} \times \tfrac{1000L}{m^3} \times 10^6$$

$$= 5.869 \times 10^{-4}\tfrac{1}{mmHg}$$

we can have a prediction of change of chemical shift induced by oxygen as shown in Figure 2-3.
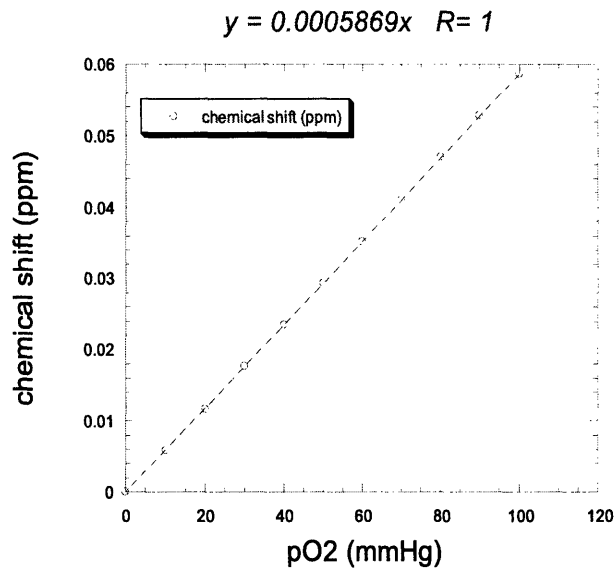
Figure 2-3: The predicted chemical shift induced by paramagnetic molecular oxygen within tissue oxygenation ranges between 0 mmHg to 100 mmHg.

In a sample such as biological tissue, it is convenient to express the Larmor frequency as

$$\omega_{eff} = \gamma B_{eff} \qquad (2.7)$$

where ω_{eff} is the effective Larmor frequency and B_{eff} is the effective magnetic field. The B_{eff} can be obtained from three factors: the magnetic field gradient, the BMS effect from paramagnetic molecular oxygen and the chemical shielding tensor. The magnetic field gradient can be written as vector,

$$G = \left(\frac{\partial B_z}{\partial x}, \frac{\partial B_z}{\partial y}, \frac{\partial B_z}{\partial z} \right) \qquad (2.8)$$

The BMS effect from paramagnetic molecular oxygen can be expressed as $[O_2]\chi_{O2}$. The chemical shielding tensor, σ, for the water protons is modified by biological factors such as pH and temperature. The chemical shielding tensor can thus be expressed as

$$\sigma = \sigma_0 + \sigma_{pH} + \sigma_T \qquad (2.9)$$

where σ_0 is the standard chemical shielding tensor caused by molecular environment, σ_{pH} is the chemical shielding tensor influenced by pH and σ_T is the chemical shielding tensor influenced by temperature. The chemical environment parameters such as pH and temperature can affect the shielding tensor because the water protons can undergo chemical exchange processes by giving up or obtaining another proton from the environment. Therefore, we can express O_2 paramagnetism for changing bulk and or specific chemical shifts as

$$B_{eff} = B_0(\Delta G + [O_2]\chi_{O2} + \sigma) \qquad (2.10)$$

Thus, in order to convert an observed chemical shift into a pO_2 we must know the effects of temperature and pH, as well as the intrinsic changes due to B0 inhomogeneities. The latter includes both the intrinsic inhomogeneity of the applied magnetic field, as well as other gradients that may be induced due to tissue compo-

31

sition and geometric factors. We propose later a method for taking such factors into account.

2.3   Paramagnetism and relaxivity

2.3.1   Relaxivity

The net macroscopic magnetization of proton spins, which is aligned parallel with the applied field along the z axis, is perturbed by application of one or more radio frequency pulses. The component of the magnetization along the z axis relaxes back to its equilibrium value with an exponential time constant, T1, the longitudinal or spin lattice relaxation time. The figure 2-4 is taken from www.cis.rit.edu/htbooks/mri. The equation that describes this behavior is:

$$M_z = M_0(1 - e^{\frac{-t}{T_1}}) \tag{2.11}$$
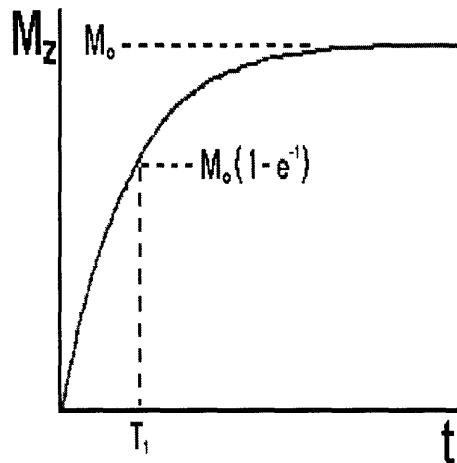
Figure 2-4: T1 is the time to reduce the difference between the longitudinal magnetization (M_z) and its equilibrium value by a factor of e.

The time dependence of the magnetization perpendicular to the z axis is characterized similarly by T2, the transverse or spin-spin relaxation time. The figure 2-5 is taken from www.cis.rit.edu/htbooks/mriinside.htm. It demonstrates the effects of

increasing the echo time, TE, upon the decay of the transverse magnetization to its equilibrium value of zero.

$$M_{xy} = M_{xy0}(e^{\frac{-t}{T_2}}) \tag{2.12}$$
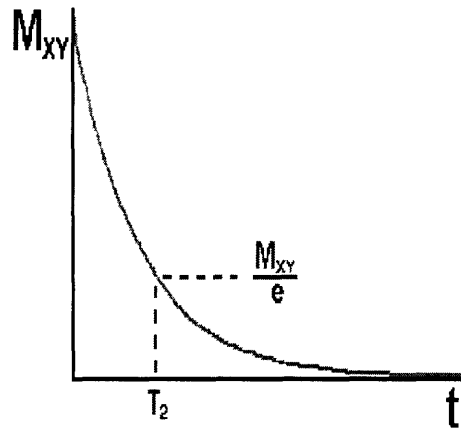
Figure 2-5: The time constant which describes the return to equilibrium of the transverse magnetization, M_{xy}, is called the spin-spin relaxation time, T2.

There are two factors affecting the decay of transverse magnetization. The first one is the pure T2 molecular effect of the molecular interactions. The second one is the variation in B_0 which leads to an inhomogeneous T2 effect. The combination of these two factors contributes the actual decay of transverse magnetization. The combined time is called T2*. The relationship between T2* and the inhomogeneities in the magnetic field can be described as the following equation

$$\frac{1}{T2*} = \frac{1}{T2} + \frac{1}{T2inhomo} \qquad (2.13)$$

The spin-spin relaxation time, T2, is the time to reduce the transverse magnetization by a factor of e. T2 and T1 processes are shown separately; however, in reality, both processes occur simultaneously and T2 is always less than or equal to T1.

Paramagnetic species can also cause an increase in the longitudinal and transverse relaxation rates, 1/T1 and 1/T2, respectively. Time-dependent fluctuations of the magnetic field resulting from the unpaired electrons provide relaxation mechanisms that give rise to shorter T1 (longitudinal) and T2 (transverse) relaxation times and, in the case of T2, linebroadening. This can be described with the following equations,

$$Ti^-1 = Ri = Ri(0) + (Ri)_p \qquad (2.14)$$

Ti^-1 is the reciprocal of the relaxation time when i=1 is the longitudinal relaxation and i=2 is the transverse relaxation. Thus, the relaxation time is the sum of the value measured in the absence of the paramagnetic agent, $Ri(0)$, and the enhancement caused by the presence of the agent, $(Ri)_p$ in which p represents paramagnetic agent. The enhancement can also be expressed as the product of hyperfine relaxivity, Ri, and the concentration of the agent [CA], as in the equation

$$Ri[CA] = (Ri)p = (Ri)_{is} + (Ri)_{os} \qquad (2.15)$$

where $(Ri)_{is}$ is the innersphere contribution or the Fermi contact interaction and $(Ri)_{os}$ is the outer sphere contribution or the dipolar interaction. More specifically, we can express oxygen as our contrast agent and since the relaxation rates are additive,

we can rewrite the equation as

$$R' = R + rC \tag{2.16}$$

where r is the specific relaxity, which describes how much the contrast agent changes relaxation rates per molar concentration.

Thus, measurement of change in relaxation time, T1, T2, T2*, may provide another value by which to characterize the O_2 concentration. The Solomon-Bloembergen (SB) equations describe the sum of scalar and dipolar contributions to relaxation time in a comprehensive way [5] [27]. As mentioned in chapter one, however, both T1 and T2 measurements are often affected by so many biological factors that their unique determination with regards to the oxygen concentration is fraught with difficulty.

Chapter 3

Methods

3.1 Introduction

The technique we are proposing is to use molecular oxygen as a contrast agent because of its paramagnetic properties and its direct effects on the relaxation of water protons, as well as its effects on bulk magnetic susceptibility. Molecular oxygen has a positive mass magnetic susceptibility and can be considered to act as a contrast agent relatively uniformly distributed in the MRI voxel. The idea is to design high-resolution NMR experiments to reveal O_2-induced chemical shift perturbations and support the oxygen level change with R2* measurements [2]. As mentioned above, there are many potential confounds in trying to assign a change in chemical shift to O_2. If we can control pH and temperature to be constant and ΔB_0 from non-oxygen sources to be as close to zero as possible, the chemical shift we observe will be mainly affected by oxygen level. The chemical shift and linewidth of different brain metabolites and water will be observed with different oxygen percentages. We will measure the chemical shift of water in the brain as well as those of other neurochemicals because some of these may reflect tissue compartmentation, allowing us to examine whether there are sub-voxel level changes in oxygen. For instance, N-acetylaspartate is found only in neurons and is synthesized in the mitochondria. Myo-inositol is found predominantly in glial cells. In addition, many of the other neurochemicals in the brain have much lower self-diffusion coefficients than water, thus they will experience less loss of phase

coherence as a result of diffusion through local tissue magnetic field gradients and will have less susceptibility change based upon the BOLD mechanisms described above. Finally, molecules such as NAA are often used as standards in measurement of brain temperature via differences between the water and NAA resonance since the latter is relatively unaffected by temperature.

3.2   Measurement of chemical shift and linewidth

Magnetic resonance spectroscopy experiments were performed on Sprague-Dawley rats which weighed between 250mg to 300 mg under 1.5 percent halothane according to guidelines of care established by the Research Review Board of the Massachusetts General Hospital.

3.2.1   Free breathing

In these experiments we measured various MR parameters as a function of inspired O_2 concentration. Thus, we performed graded hypoxia and hyperoxia experiments. We simultaneously measured the arterial oxygen saturation (SaO_2) using pulse oxymetry and the relationship between FIO_2 (fraction inspired oxygen) and SaO_2. For each rat, we ran two spectroscopy scans to get water suppressed and water unsuppressed data and we ran one gradient echo experiment to determine changes in R2* [30]. Thus, for each oxygen level, there are three sets of data. The water-suppressed spectra consisted of brain metabolite chemical shifts and linewidths. The second, unsuppressed, water spectra allowed for measurement of the water chemical shift and linewidth. The third experiment was a gradient echo experiment to give us the signal average and change in R2*. We used a PRESS (point resolved spectroscopy sequence) pulse sequence for the spectroscopy experiments [6]
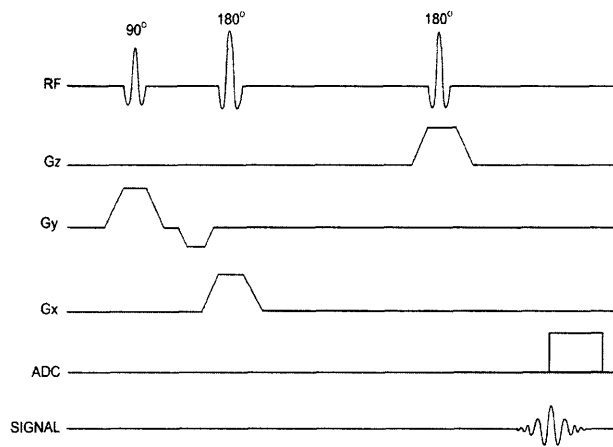
Figure 3-1: Single-voxel PRESS pulse sequence timing diagram. It uses a 90180180 pulse train and detects the spin echo following the second 180 pulse. The image is taken from Figure 21 of [6].

and shimmed it with the FASTMAP [14] tool provided by BRUKER. The spectroscopy data can be run with a short echo time which minimizes the BOLD effects based upon changes in local deoxyhemoglobin concentrations. The basic sequence comprises one selective 90 radiofrequency RF pulse followed by two slice selective 180 pulses. All three pulses are mutually orthogonal. The three pulses generate an echo from a single region at the intersection of these planes. The experiments were performed on either 4.7 T or 9.4 T. The data was fit with Nuts 1-D NMR program to obtain the brain metabolites' linewidth and peak position.

3.2.2 Ventilation

In order to gain better control of the animals respiration, and hence more stability in the oxygen values, we performed a ventilation technique on the rats. Male rats (250-325 gm) were anesthetized with 1.5 percent halothane in oxygen for insertion of femoral arterial and venous cannulae and placement of tracheal catheter for mechanical ventilation (16 gauge intravenous catheter). All wounds were infiltrated with 1 percent lidocaine before incision. Following surgery, the inspired halothane concentration was reduced to 1 percent and the rats were paralyzed with 2 mg/kg intravenous pancuronium, followed by a continuous intravenous infusion of 2 mg/kg/hr. Rats were mechanically ventilated (small animal volume controlled ventilator, Harvard Apparatus, Inc.) with a 2/1 liter per minute oxygen/nitrogen mixture, an inspiratory to expiratory ratio of 1:1, and an initial tidal volume of 4.0 ml at a rate of 40 breaths per minute. Ventilation parameters were adjusted to maintain normal arterial blood gases (pH = 7.40 0.01, $PaCO_2$ = 40 2, PaO_2 = 145 10). Rat torsos were wrapped in two heating blankets (Gaymar, Orchid Park, NY) circulating warm water to maintain core temperature at 37-38 C. In order to minimize MRI motion artifact, rats were placed into a custom plastic cradle attached to a head frame machined from delrin plastic; heads were fixed with plastic ear bars and a bar inserted under the front incisors. After placing an MRI surface coil over the head, the animals were positioned in the magnet center. Blood pressure (from arterial catheter), heart rate (from A-line and pulse oximeter), arterial oxygenation (pulse oximeter), and body temperature

were monitored continuously to assess anesthetic depth and physiological stability. MRS experiments then performed on rats in 4.7T or 9.4T as described in the above section. The oxygen level was varied from 16 percent to 100 percent throughout the time of the experiment in a steady increase or decrease.

3.3   Standardize chemical shift

An internal reference was needed to process spectroscopy data. We tested three different methods to standardize chemical shift. At first, we decided to use lipid from the scalp as an internal reference since it is not well-perfused with blood and hence has very low oxygen delivery. Thus, its chemical shift should not change much with inspired O_2 concentration. We also ran some experiments with phantoms to use as an external reference. The phantoms were made from saline or 2 percent agar. The solution was then poured into a 1 ml syringe or a 6 ml syringe. The phantom was placed on top of the surface coil atop the rat's head. The water chemical shift from the phantom was analyzed with the Nuts 1-D NMR program. The last technique that was used to standardize the chemical shift was to scale the NAA chemical shift with 100 percent oxygen. The scaled result was around 2.046 ppm. We chose 100 percent oxygen as our standardizing point because at 100 percent, the change in physiological environment should be the same for all animals and tissue should be saturated with oxygen. Thus, it was reasonable to use 100 percent as the point to scale all the spectroscopy data.

3.3.1   Brain temperature

The temperature dependence of the water proton chemical shift could also be used to monitor the stability of brain temperature throughout the experiments. According to [8], in vivo brain temperature could be analyzed by examining the difference between NAA chemical shift and water chemical shift.

$$T = 286.9 - 94(\delta_{water} - \delta_{NAA}) degreeCelcius \qquad (3.1)$$

Therefore, we also measured the difference between NAA and water chemical shift to ensure that the temperature changes were not a major cause of the effects we observed.

3.4 Gradient echo experiment

We performed a gradient echo experiment to determine changes in R2* and confirm the oxygen change in tissue. We used the gradient echo signals with various oxygen percentages to validate that there was a change in tissue oxygenation during each experiment. The gradient echo experiments were performed with 4.7 T or 9.4T (Bruker) after acquiring brain metabolite and water spectroscopy using a TE=10 ms and TR=600ms. A single loop surface coil was used for radio frequency transmission and reception.

Chapter 4

Results

4.1 Measurement of chemical shift and linewidth

Throughout each experiment, we used a pulse oximeter to monitor the physiological status of the rats. We collected SaO_2 (arterial saturation of oxygen) for every experiment. Figure 4-2 showed that there is a sigmoid relationship between SaO_2 and FIO_2. The saturation point was around 30 percent of FIO_2. In other words, all the hemoglobin was bound with oxygen after 30 percent. Thus, after 30 percent, the paramagnetic effect is dominated by that from molecular oxygen.
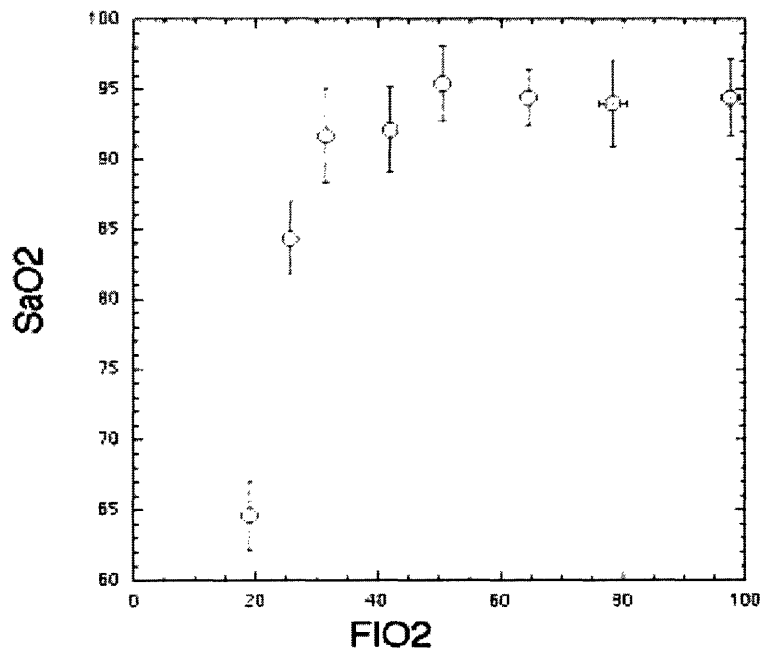
Figure 4-1: The average change in SaO_2 as a function of FIO_2 for free breathing animals. It showed a sigmoid relationship between SaO_2 and FIO_2. The saturation point is around 30 percent of FIO_2.
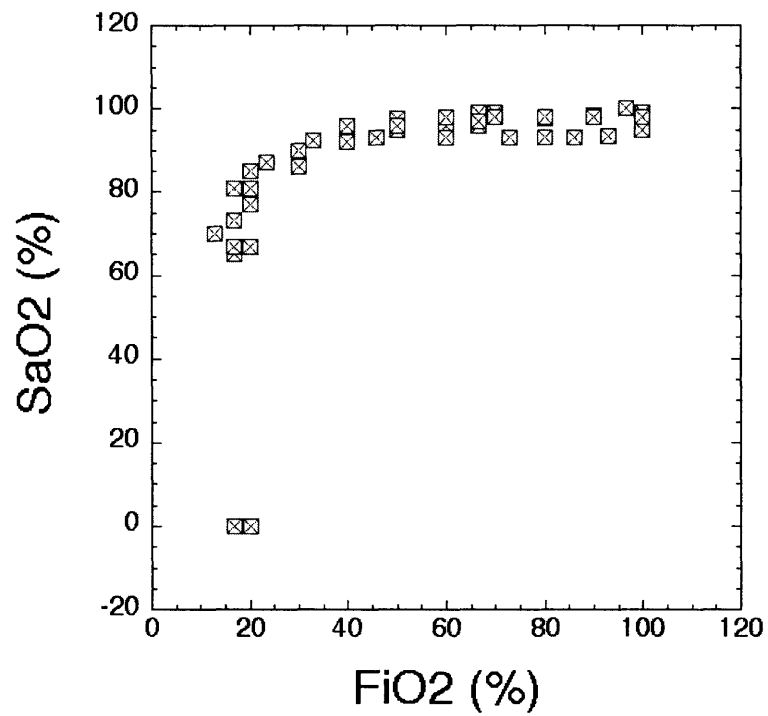
Figure 4-2: The average change in SaO_2 as a function of FIO_2 for ventilated animals. It showed a sigmoid relationship between SaO_2 and FIO_2. The saturation point is around 30 percent of FIO_2.

4.1.1 Data from free breathing animals

A representative spectrum from one of the free breathing animals is shown in Figure 4-3. We standardized the chemical shifts with NAA=2.046 ppm at 100 percent.
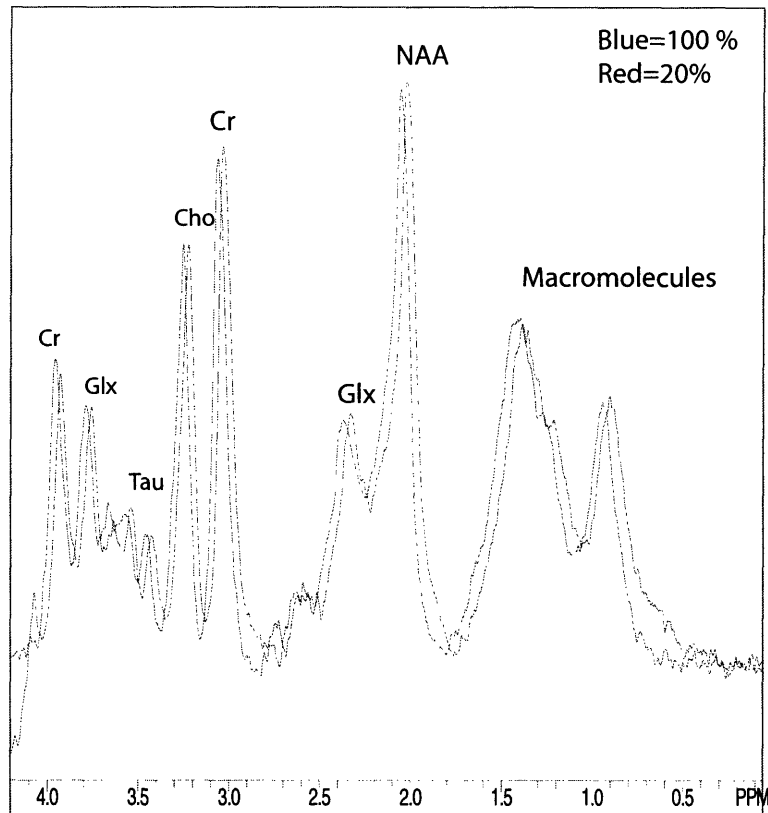
Figure 4-3: The spectra is normalized at NAA=2.046 ppm at 100 percent. TE=20 ms

Shown in Figure 4-4, Figure 4-5, Figure 4-6 and Figure 4-7 are chemical shift data as a function of FIO_2. There was a linear relationship between the FIO_2 and the chemical shift of brain metabolites and water. The changes in chemical shifts confirmed our predictions that the peak positions would have a downfield shift with higher oxygen percentage due to its paramagnetism.
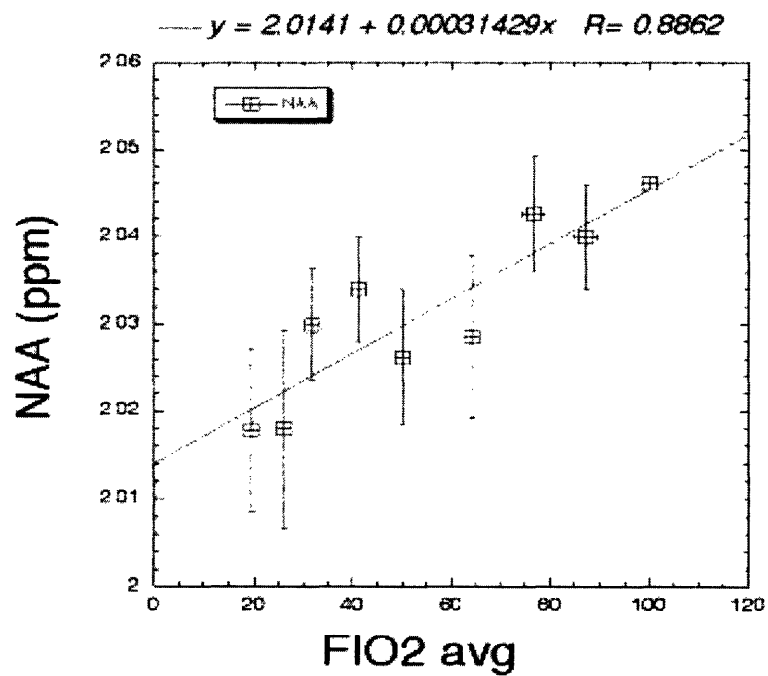
Figure 4-4: Averaged variation in chemical shift of NAA with FIO_2 from four free breathing animals
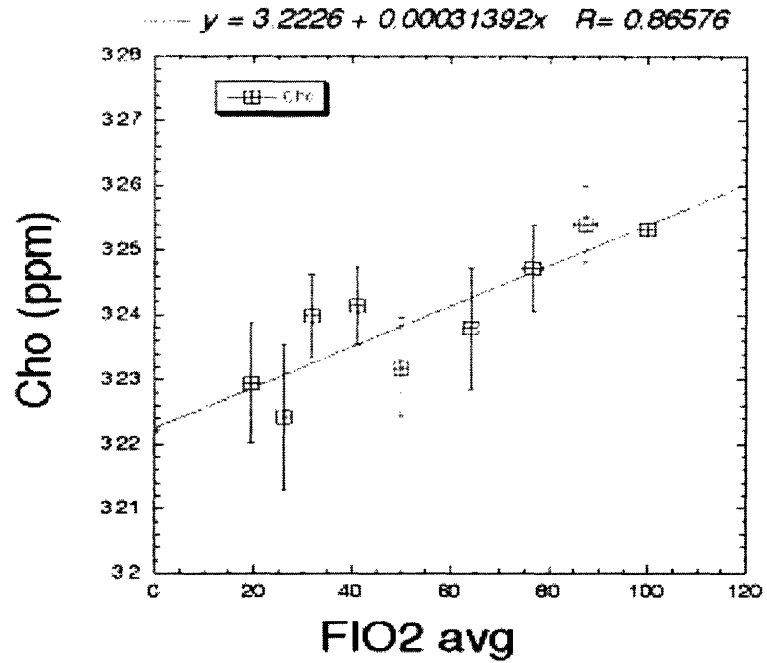
Figure 4-5: Averaged variation in chemical shift of choline with FIO_2 from four free breathing animals
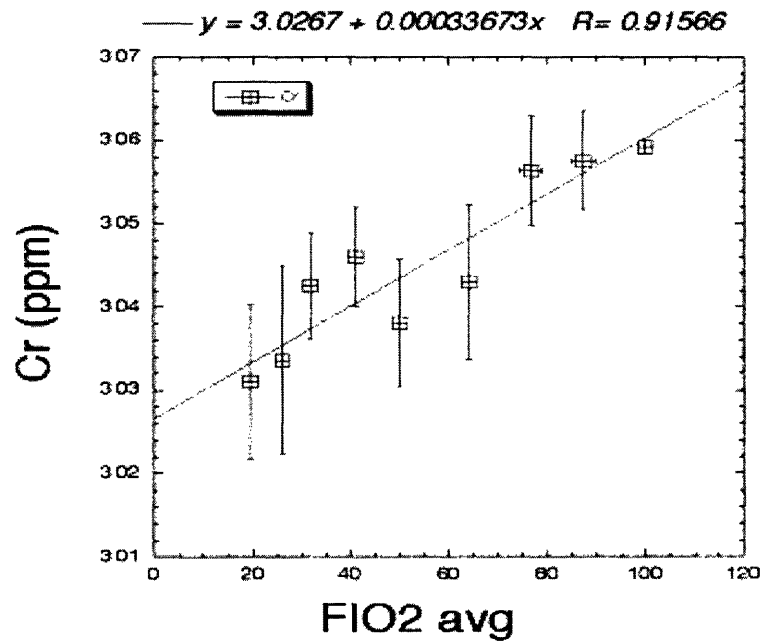
Figure 4-6: Averaged variation in chemical shift of creatine with FIO_2 from four free breathing animals
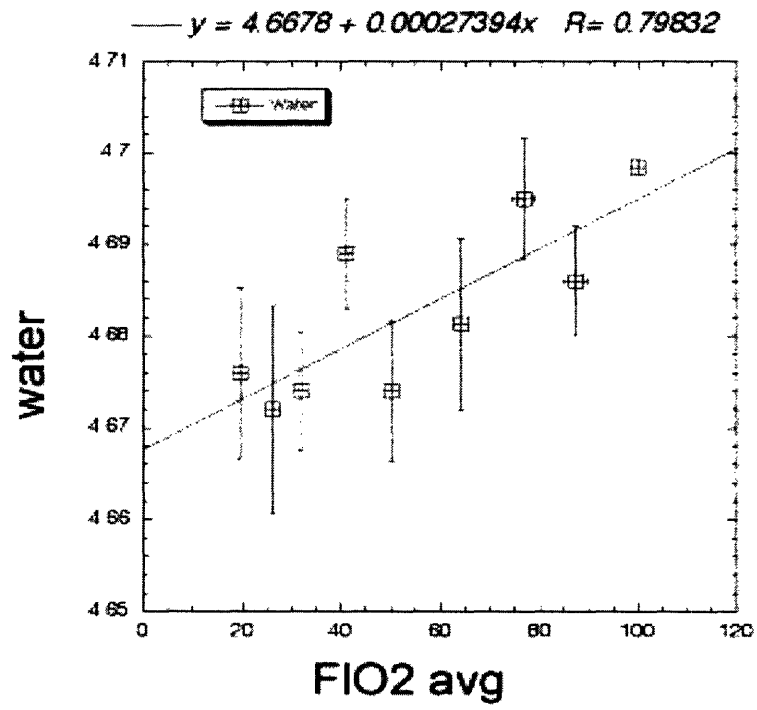
Figure 4-7: Averaged variation in chemical shift of water with FIO_2 from four free breathing animals

All the neurochemicals showed an apparently linear trend with change of oxygen percentage. Differences in the slopes were not significant.

4.1.2 Ventilation experiments

We ran the same experiment with animals under ventilation to achieve a more stable physiological preparation.

As shown in Figure 4-8, Figure 4-9, Figure 4-10 and Figure 4-11, all of them had a similar slope with variation of FIO_2. The chemical shift of brain metabolites and water had a downfield shift with increase of FIO_2 due to the paramagnetism of molecular oxygen.

$$y = 2.0151 + 0.00028178x \quad R = 0.9728$$
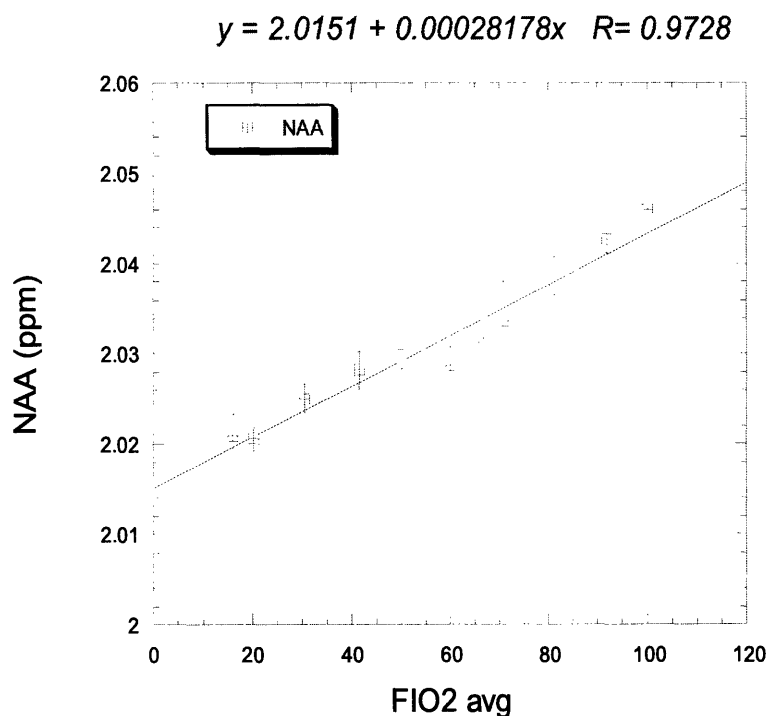
Figure 4-8: Averaged variation in chemical shift of NAA with FIO_2 from five ventilated animals

The ventilation technique offered better control in the biological system and the data were less noisy compared to free breathing data. The R square value for the slope of FIO_2 versus chemical shift was smaller for ventilation data than for free

50

$$y = 3.2129 + 0.00023882x \quad R= 0.91796$$
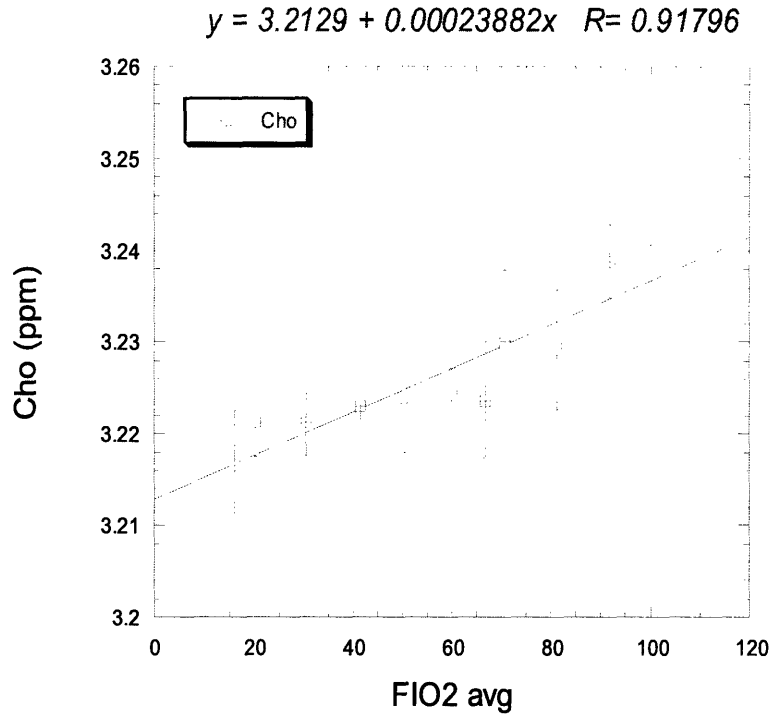
Figure 4-9: Averaged variation in chemical shift of choline with FIO_2 from five ventilated animals

breathing data as shown in Figure 4-12. However, the absolute value of the slopes was similar. The averaged slope for the metabolites and the water was close to the theoretical value. However, the relation between the FIO_2 and the pO_2 (the pO_2 was used to generate the theoretical slope) is not known. Some authors use $pO_2 = a \times FIO_2$. As a matter of fact our value of the slope would allow us to determine a as $= 0.4867$.

The results from linewidth experiments could also be interpreted in a similar manner. The observed linewidth is equal to the sum of the linewidth due to the change in concentration of the hemoglobin and the linewidth due to the change in concentration of dissolved oxygen in tissue. Thus, during the lower oxygen period, deoxyhemoglobin caused the change of linewidth and the paramagnetic molecular oxygen caused the linewidth to increase after the saturation point. We observed almost a parabolic relationship between water linewidth, averaged brain metabolite linewidth and oxygen as shown in Figure 4-13 and Figure 4-14.
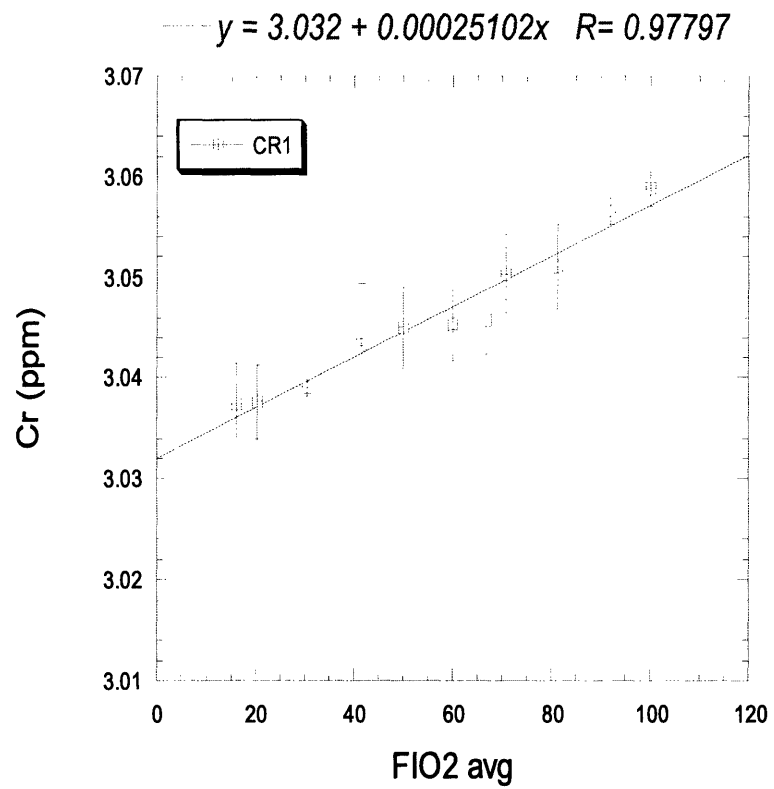
Figure 4-10: Averaged variation in chemical shift of creatine with FIO_2 from five ventilated animals

$$y = 4.6865 + 0.00027466x \quad R= 0.92603$$
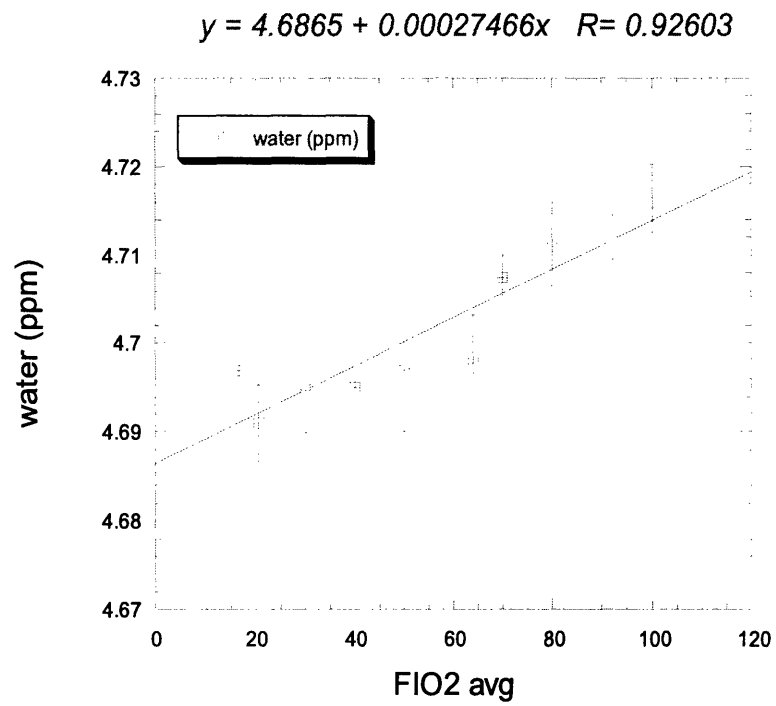
Figure 4-11: Averaged variation in chemical shift of water with FIO_2 from five ventilated animals

	Slope	R value
NAA free breathing	0.00031429	0.8862
NAA ventilated	0.00028178	0.9728
Cho free breathing	0.00031392	0.86576
Cho ventilated	0.00023882	0.91782
Cr free breathing	0.00033673	0.91566
Cr ventilated	0.00025102	0.97797
Water free breathing	0.00027394	0.79832
Water ventilated	0.00027466	0.92603
	averaged slope	theoretical slope
	0.000285645	0.0005869

Figure 4-12: Table of averaged chemical shift slope from free breathing animals and ventilated animals. The R values for ventilated animals are higher than the free breathing ones. The averaged slope for both free breathing and ventilated animals is close to the theoretical slope since $pO_2 = a \times FIO_2$.
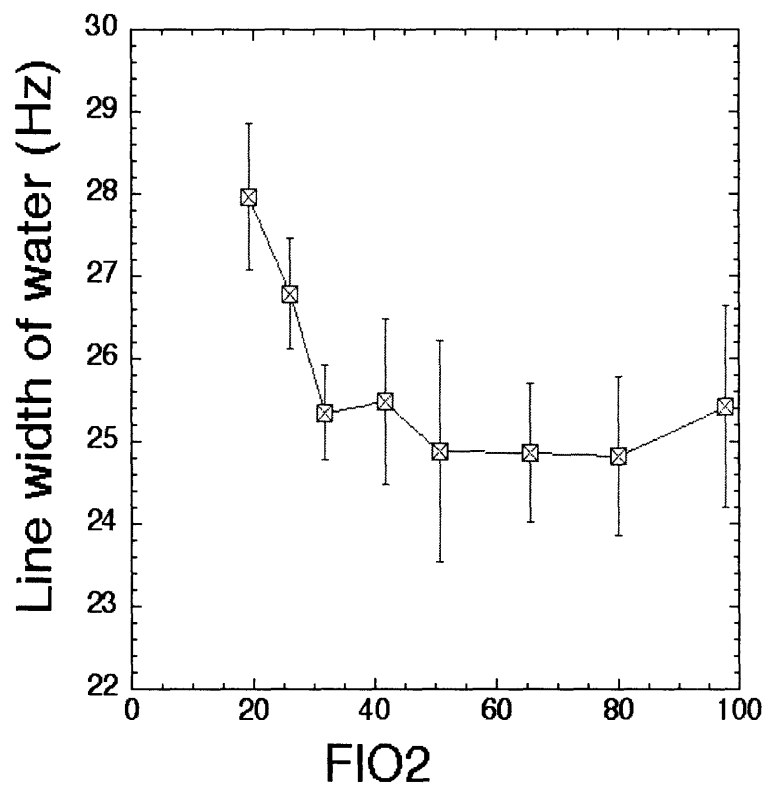
Figure 4-13: Averaged water linewidth with FIO_2 shows a parabolic relationship.

Average Brain Metabolite Linewidth vs. FIO2
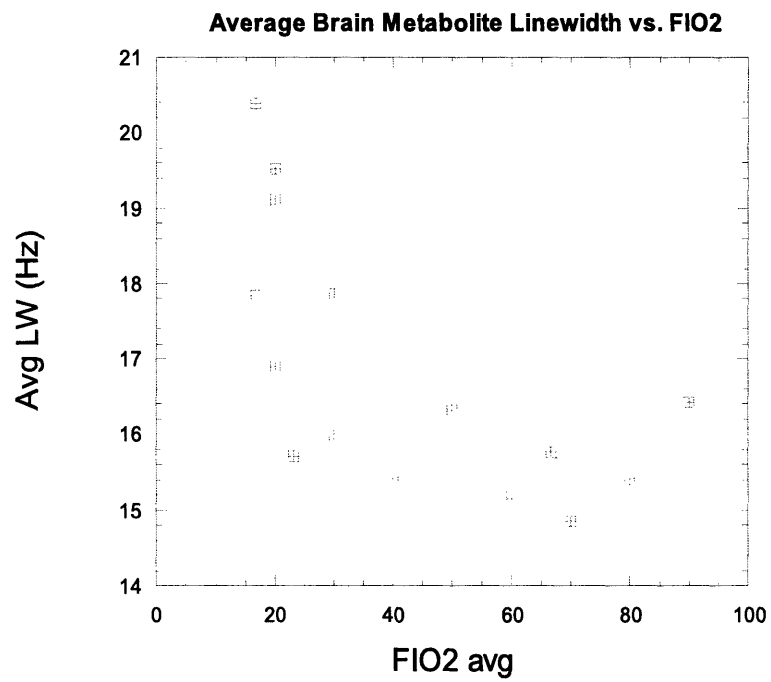
Figure 4-14: Averaged brain metabolite linewidth with FIO_2 shows a parabolic relationship.

4.1.3 Use lipid as an internal reference

At first, we decided to use scalp lipid to standardize our chemical shift. We used it as an internal reference because it is not well-perfused with blood and hence had a very low oxygen delivery. Also, we can have scalp lipid as a control to see whether or not the effects of increased oxygen in the air around the head leads to changes in the magnetic susceptibility and changes of chemical shift that we observe in the brain. The chemical shift did not change much with inspired oxygen concentration. This was shown in Figure 4-15.

$y = 1.5104 + 3.6069e{-}06x \quad R = 0.043896$
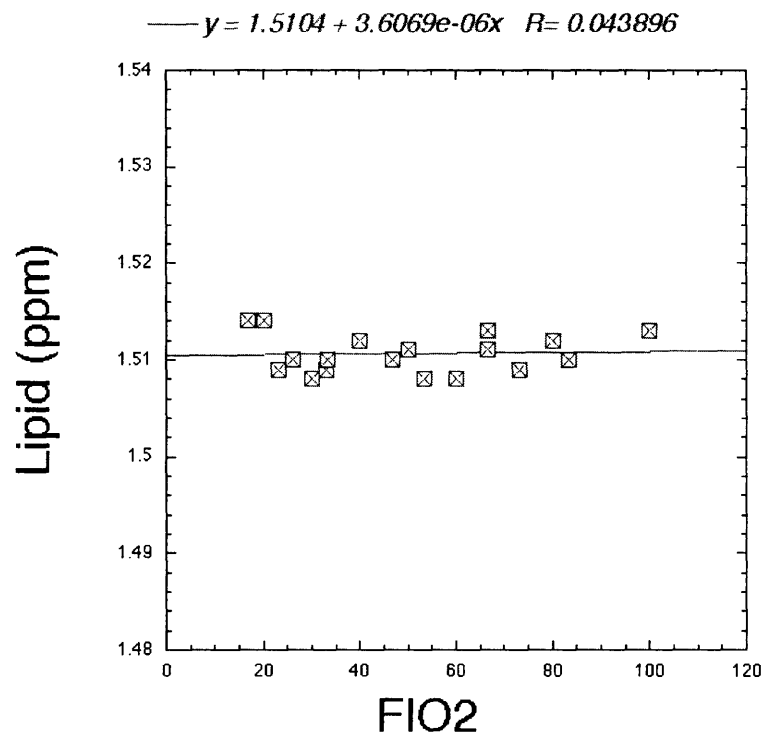
Figure 4-15: Lipid chemical shift with FIO_2. The correlation is low and shows that there is no significant chemical shift with various FIO_2.

4.1.4 Use of a phantom as an internal reference

Another possible internal reference could result from using a phantom. The phantom serves two purposes. First, it provides a chemical shift standard. Second, it controls for the effects of increased oxygen in the air around the head leading to changes in the magnetic susceptibility that would affect the brain water and metabolite chemical shifts. The phantom water spectra was analyzed by the 1-D Nuts program and standardized with 100 percent NAA peak position to reserve the consistency of data analysis for brain metabolites. As shown in Figure 4-16, the phantom water had a very small slope with change of FIO_2. If we compared it with brain water chemical shift as shown in Figure 4-17, we could see very clearly that phantom water chemical shift did not vary with different oxygen levels while brain water did.

Average Change in Water Chemical Shift in Phantoms

$y = 4.7454 + 1.0703e\text{-}05x \quad R^2 = 0.028975$
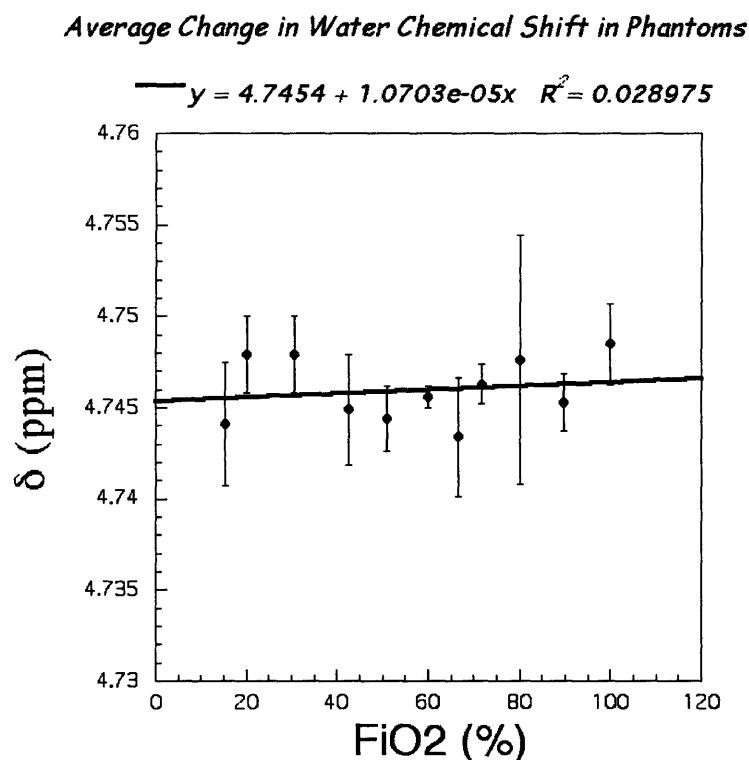
Figure 4-16: Averaged phantom water chemical shift with FIO_2 from four experiments. The correlation is low and shows that there is no significant chemical shift with various FIO_2.

58

$y = 4.7194 + 1.0703e\text{-}05x \quad R^2 = 0.028975$

$y = 4.6842 + 0.00029736x \quad R^2 = 0.90334$
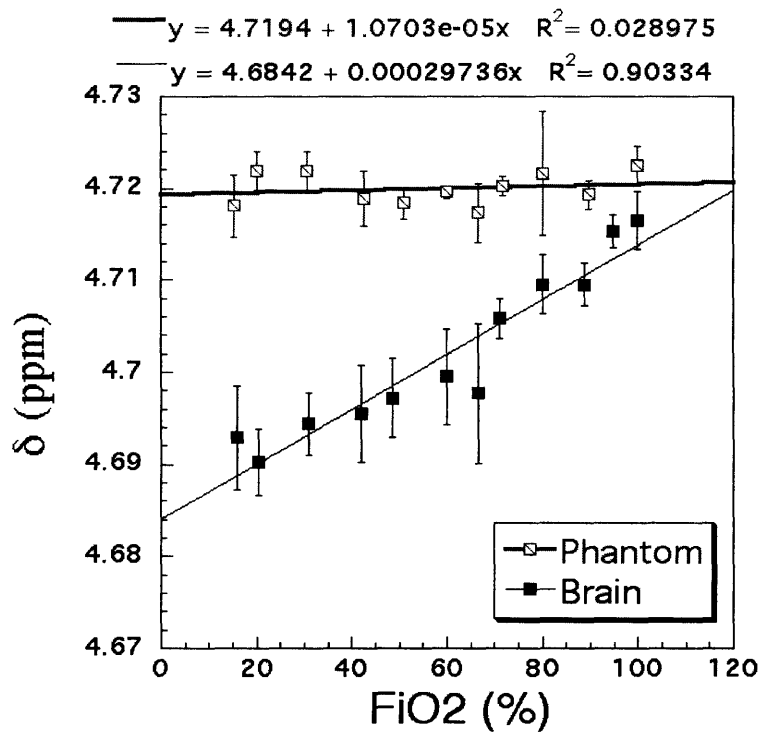
Figure 4-17: Averaged phantom water chemical shift compared with averaged brain water chemical shift with variation in FIO_2. Brain water chemical shift has a significant slope while phantom water chemical shift has a relatively flat slope.

59

4.1.5 Brain temperature

By calculating the difference in chemical shift of water and NAA [8], we obtained brain temperature information with various FIO_2. As shown in Figure 4-18, the correlation was small between brain temperature and FIO_2. Also, the brain temperature was very stable and did not show much change during the experiments.
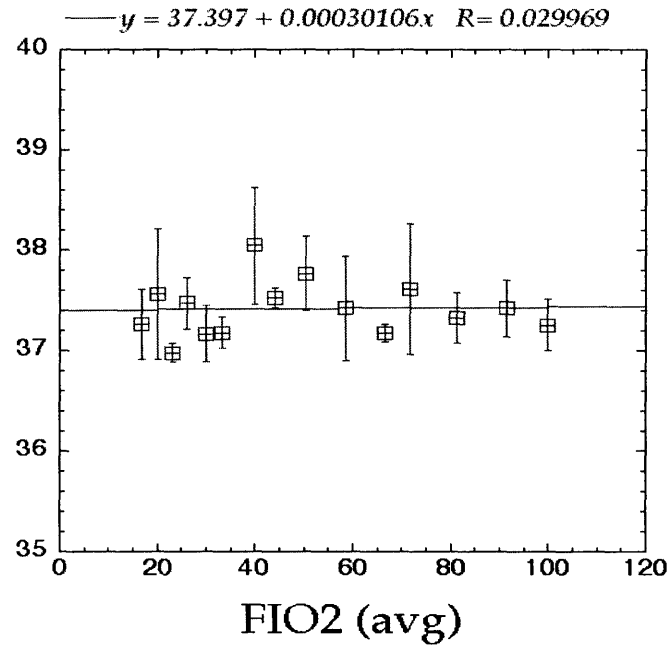
Figure 4-18: Averaged brain temperature with various FIO_2. The correlation was low between brain temperature and FIO_2.

4.2 Gradient echo experiments

The third part of the experiment was to obtain gradient echo signals as a function of inspired oxygen concentration to validate that there was a change in tissue oxygenation during each experiment. As shown in Figure 4-19, there was a very good correlation between gradient echo signals and SaO_2 and the result agreed with previous studies [3]. As shown in Figure 4-20, there was an exponential increase of gradient echo signals with SaO_2 and with signals from the arteries. Figure 4-19 showed a very good correlation between gradient echo signals and SaO_2.
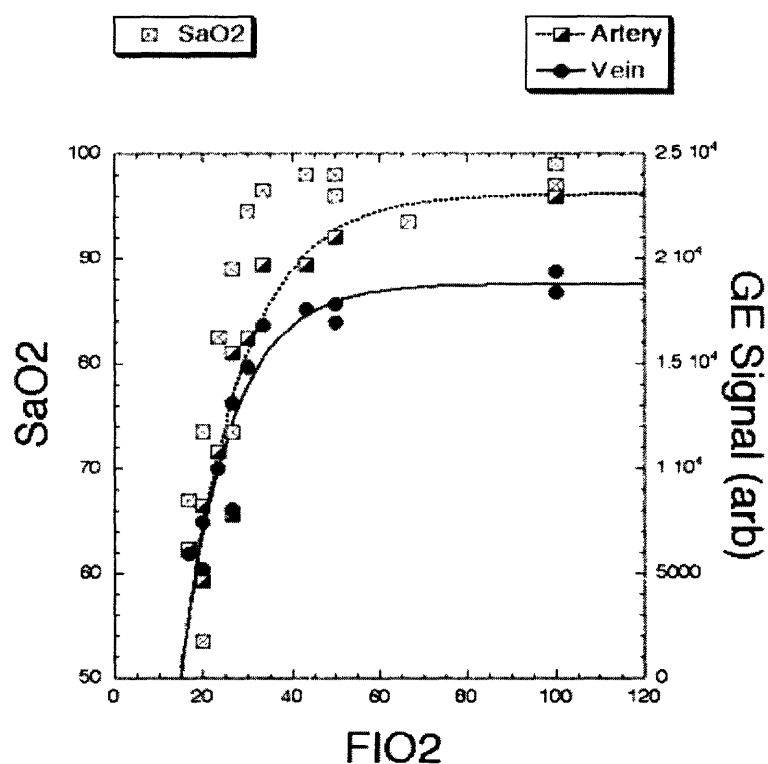
Figure 4-19: The gradient echo signals from voxels containing predominantly artery or vein were compared with SaO_2 and FIO_2.

We also used this equation to obtain R2*=1/T2* values.

$$\Delta R2* = -ln(\frac{S}{S0}) * (\frac{1}{TE})$$

(4.1)

We used the signal intensities from FIO_2=100 percent as the baseline, S0, to
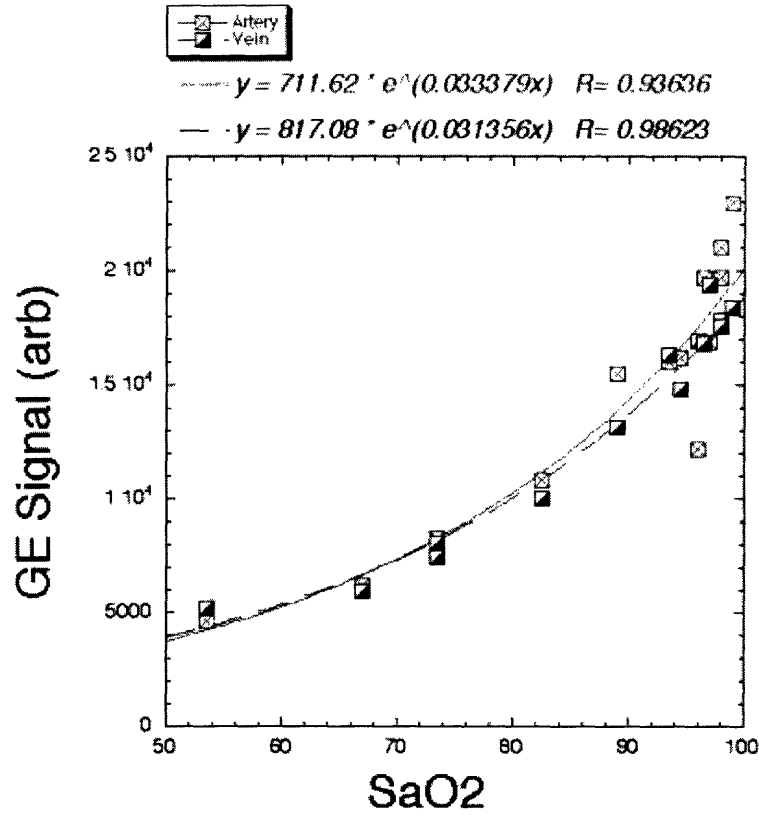
Figure 4-20: Gradient echo signals from artery and vein show an exponential increase of SaO_2.

obtain the R2*. The relationship between blood hemoglobin oxygen saturation and the apparent transverse relaxation rate R2* can be defined as [18]:

$$R2* = \frac{1}{T2_0*} + A(1-Y) + B(1-Y)^2 \qquad (4.2)$$

where $T2_0*$ is the T2* of fully oxygenated blood, Y is the fraction of oxygenated hemoglobin in blood, and A and B are the coefficients of a linear dependence of R2* on (1-Y) reflecting the static spin-dephasing effect of deoxyhemoglobin and a quadratic dependence on (1-Y) reflecting the diffusion effects.

As shown in Figure 4-21 and Figure 4-22 and Figure 4-23, the R2* would be increased at the lower oxygen region due to paramagnetic deoxyhemoglobin. Also, R2* was very sensitive to paramagnetic deoxyhemoglobin since it had the greatest

changes at the lower oxygen region. R2* also fit better with SaO_2 since the R square values were slightly higher. R2* decreased exponentially with FIO_2 while decreasing linearly with SaO_2.
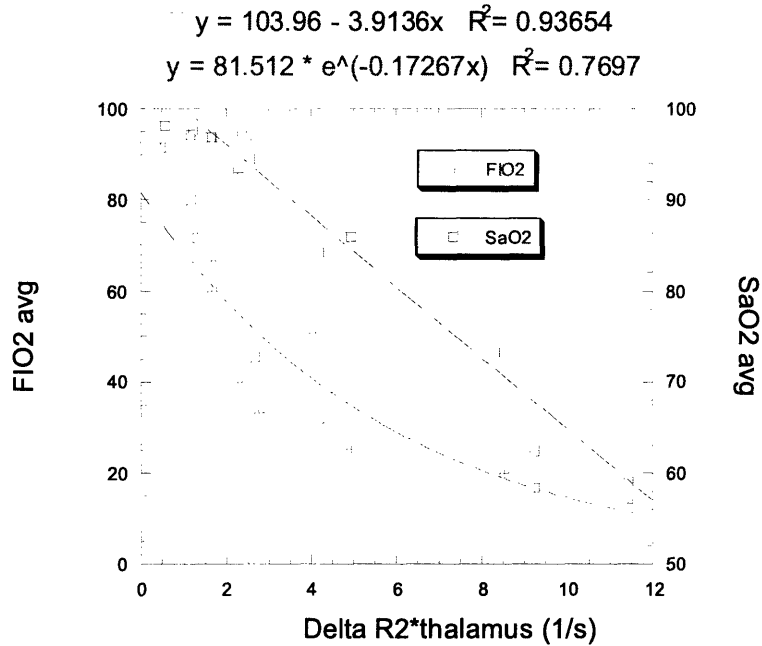
$$y = 103.96 - 3.9136x \quad R^2 = 0.93654$$
$$y = 81.512 * e^{\wedge}(-0.17267x) \quad R^2 = 0.7697$$

Figure 4-21: The Δ R2* values from 4.7 T showed an exponential decrease with FIO_2 and a linear decrease with SaO_2.

There was a larger change in R2* in the artery region because the artery was very sensitive to oxygen change and thus would cause a bigger reduction in R2*.
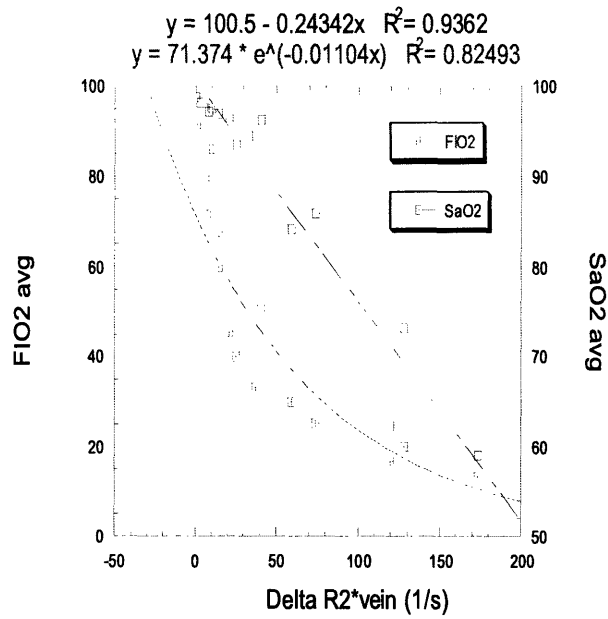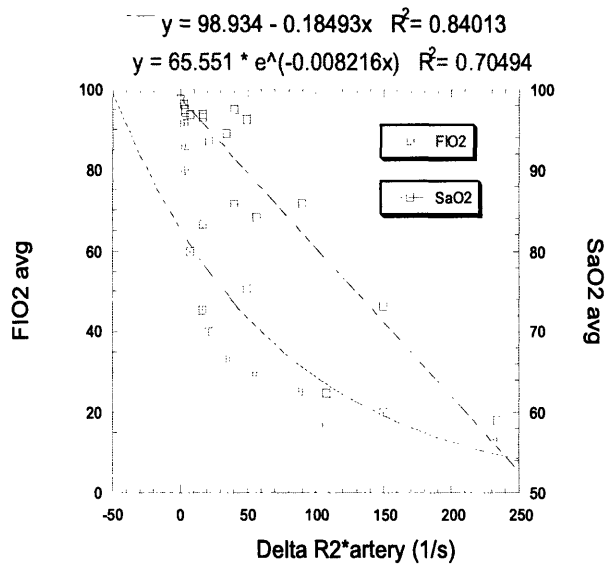
Figure 4-22: The Δ R2* values from 4.7 T showed an exponential decrease with FIO_2 and a linear decrease with SaO_2.

Figure 4-23: The Δ R2* values from 4.7 T showed an exponential decrease with FIO_2 and a linear decrease with SaO_2.
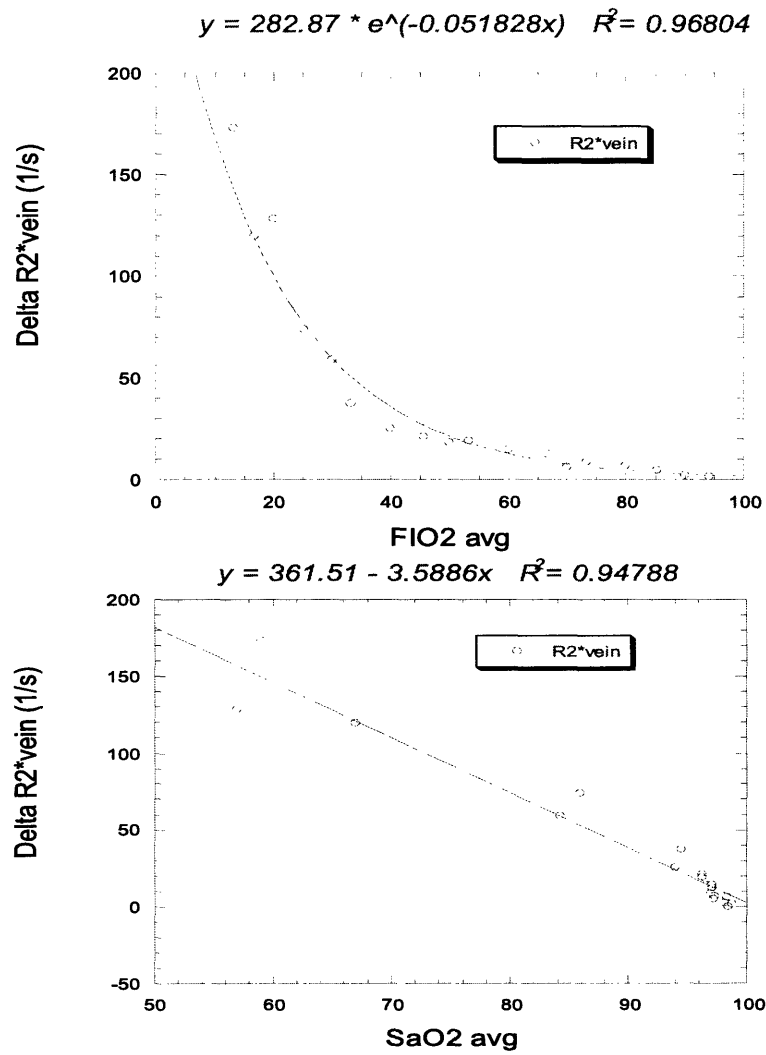
$$y = 18.337 * e^{\wedge}(-0.044088x) \quad R^2 = 0.90341$$

$$y = 26.324 - 0.25695x \quad R^2 = 0.94927$$

Figure 4-24: The Δ R2* value showed an exponential decrease with FIO_2.

Figure 4-25: The Δ R2* value showed an exponential decrease with FIO_2.

$$y = 298.77 * e^{(-0.053211x)} \quad R^2 = 0.86124$$

$$y = 422.48 - 4.189x \quad R^2 = 0.8532$$
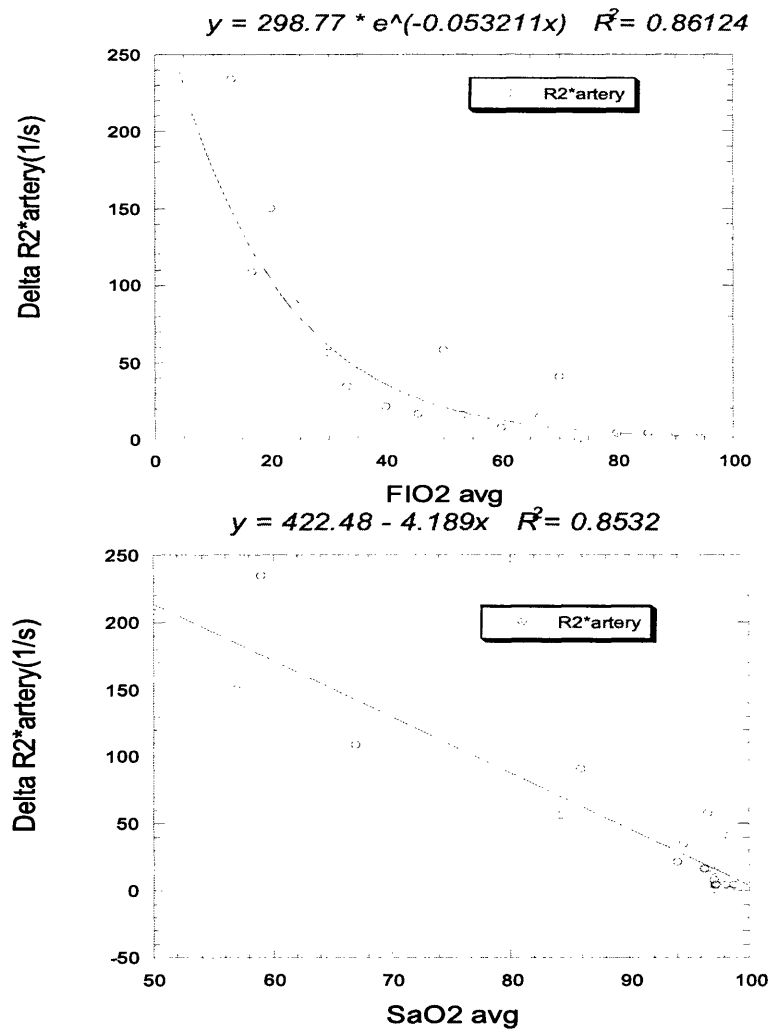
Figure 4-26: The Δ R2* value showed an exponential decrease with FIO_2

Figure 4-24 and Figure 4-25 and Figure 4-26 showed the R2* data from 9.4 T scanner. The 9.4 T data demonstrated the same trend between FIO_2, SaO_2 and R2*. The change in R2* range was bigger because of higher magnetic strength.

Chapter 5

Summary

5.1 Discussion and conclusion

The goals of this thesis are to test our hypothesis that magnetic resonance spectroscopy (MRS) can be used to measure tissue oxygenation, to compare this technique with the popular BOLD technique by measuring R2* with gradient echo experiments and to explore the possibilities of implementing this technique in clinical practice.

Both free breathing and ventilated rats showed the same downfield trend for chemical shift change with increased FIO_2 and had similar slopes. However, ventilated animals had a better correlation with FIO_2 and smaller error bars. Thus, ventilation proved to provide better control in the biological system. Brain metabolite slopes showed no different slope from the water slope and thus indicated little effect of compartmentalization on the effects of molecular oxygen. By obtaining brain temperature data from NAA chemical shift and water chemical shift, the chemical shift that we observed from various FIO_2 level was not due to the temperature fluctuation because the temperature was stable throughout the experiments and showed no correlation with FIO_2.

Scalp lipid proved to be a very good possible internal reference due to its low perfusion and hence low change in chemical shift with FIO_2. Phantom proved to be a better internal reference choice and the water chemical shift from phantom showed no correlation with FIO_2.

Gradient echo experiments demonstrated R2* was very sensitive to SaO2 changes. Despite its major advantage of being quite simple and providing high sensitivity at low oxygenations, the disadvantage is the complexity of signal interpretation in terms of its relation to pO_2 change. At the lower oxygen saturations, R2* had a large change with only a little change in FIO_2 or SaO2 values. It might seem attractive to simply run gradient echo experiments and measure the change of R2* values to coordinate with tissue oxygenation. However, the change in R2* values was confounded due to the combination of oxygen consumption and blood flow, and we could not quantify the oxygen level with the change of R2* values. Nonetheless, the gradient echo BOLD data served to show that the changes we observed in chemical shift as a function of FIO_2 were likely due to changes in tissue oxygenation. Future studies will involve use of invasive MRI-compatible oxygen electrodes to verify the sensitivity to tissue oxygenation.

The results showed a very promising possibility for using chemical shift as an oxygen sensor. Most encouraging was that the actual slopes attained from the measurements of the metabolites were fairly linear with FIO_2 (and hence tissue pO_2) and the absolute values of the slopes we obtained were quite similar to those predicted from simple use of Henry's law and the known paramagnetic susceptibility of oxygen. However, like other techniques, our method suffered some difficulties too. Although the ventilation technique proved to reduce some biological error, we would like to work on reducing the error bars. Interestingly, in a subset of animals (n=2) where the experimental quality was extremely high, we obtained slopes closer to the theoretical prediction. The differences between these animals and the majority of the other animals remains to be investigated.

5.2 Directions for future research

5.2.1 Implementation in stroke and tumor models

Two very important clinical conditions in which knowledge of tissue pO_2 is vital are strokes and tumors. Our technique could likely serve as an important adjunct to current methodologies. Hypoxia is known to exist in certain brain tumors. High oxygen levels are crucial for effective radiation therapy because radiation kills tumor cells by forming oxygen radicals - highly reactive oxygen atoms that damage DNA. Chemotherapy might be affected by the fluctuations because if tumor blood flow drops, the drugs might not be delivered efficiently throughout the tumor. Thus, tumor tissue will have a different oxygenation environment from the normal tissue and our technique can be well applied to measure the tumor oxygenation. The idea can be illustrated in Figure 5-1.

Figure 5-1: An illustration of the tumor tissue in the brain

The idea is to take the voxel in a normal tissue region near the tumor tissue and take another voxel in the tumor tissue. Most tumor tissues have low oxygen levels because of lack of oxygen delivery. We can use the normal tissue's chemical shift induced by oxygen as the baseline and predict the oxygen level of the tumor from our method. We will first determine the normal tissue oxygen level by varying the oxygen level to obtain at least two different oxygen points so we can linearly fit and obtain our normal tissue oxygen level. Then we can obtain the difference in chemical shift of normal tissue and tumor tissue to obtain the oxygen level of the tumor tissue.

$$\delta_{normal} - \delta_{tumor} = \chi_{O2} pO_2 \qquad (5.1)$$

The same procedure can also apply to a stroke model to determine the tissue oxygenation in ischemic areas.

5.2.2 Future work

Future work on this project will mainly consist of improving the precision of our system and reducing the source of errors. In addition, one of the biggest problems with this technique is the B_0 inhomogeneity because all chemical shift differences increase in proportion if B_0 is increased. Thus, for instance, if one could determine the absolute chemical shift of water, independent of non-oxygen dependent B_0 changes then one could in principle use this chemical shift of water to predict the pO_2. In practice this is likely to be quite difficult. First, there are B_0 changes due to the magnetic field inhomogeneity. These are likely to exhibit smaller gradients as a function of space (i.e. dB/dx has a small value). These have the potential to be corrected for by making B_0 field maps. A more severe problem is changes in B_0 due to effects like tissue iron. This can likely be corrected by using multiple offset gradient echoes. Since the tissue water diffuses around the iron (most of which will be bound on the form of macromolecules like ferritin or hemosiderin), then the R2* contrast properties should be quite dependent upon echo time. In contrast, T2 changes due to molecular oxygen are likely to be much less echo time dependent since the molecular oxygen has high

diffusivity and will affect the dipolar T2. In our case, the B_0 is not constant throughout the human head. Thus, we can't really have an absolute change of chemical shift. We can correct this by using an external reference; however, in such cases the magnetic field B_0 for the sample is not strictly comparable with that for standard because the external reference and tissue will have different magnetic susceptibilities. Having a constant B_0 is important for our technique because chemical shift difference is very sensitive to B_0 field.Our method of using the graded hyperoxia has some attractions. First, as we showed, the technique appears to be equally sensitive across the entire range of FIO_2 values, unlike gradient echo techniques that are very insensitive at high oxygenations. Second, the anticipated slope change should be independent of the starting B_0. Thus, by measuring the slope one can predict the original pO_2.

To implement this technique in strokes or tumors, we might encounter one difficulty. We used 100 percent NAA=2.046 ppm to standardize our chemical shift data. However, for the tumor or stroke tissues, the oxygen delivery might not be efficient or not as perfused as the normal tissue and the tissue will not be saturated even with FIO_2=100 percent. Thus, with our technique of standardization of chemical shift, we might get a different -specifically a smaller- slope for stroke or tumor tissues.

Bibliography

[1] E.O. Aboagye, R.J. Maxwell, A.B. Kelson, M. Tracy, A.D. Lewis, M.A. Graham, M.R. HOrsman, J.R. Griffiths, and P. Workman. Preclinical evaluation of the fluorinated 2-nitroimidazole n-(2-hydroxy-3,3,3-trifluoropropyl-2-(2-nitro-1-imidazolyl) acetamide (sr-4554) as a probe for the measurement of tumor hypoxia. *Cancer. Res.*, 57:3314–3318, 1997.

[2] C. Baudelet, R. Ansiaux, B. F. Jordan, X. Havaux, B. Macq, and B. Gallez. Physiological noise in murine solid tumours using t2*-weighted gradient-echo imaging: a marker of tumour acute hypoxia? *Phys. Med. Biol.*, 49:3389–3411, 2004.

[3] C. Baudelet and B. Gallez. How does blood oxygen level-dependent (bold) contrast correlate with oxygen partial pressure (po2) inside tumors? *Mag. Reson. Med.*, 48:980–986, 2002.

[4] C. Baudelet and B. Gallez. Effect of anesthesia on the signal intensity in tumors using bold-mri: Comparison with flow measurements by laser doppler flowmetry and oxygen measurements by luminescence-based probes. *Magnetic Resonance Imaging*, 22:905–912, 2004.

[5] N. Bloembergen. Proton relaxation times in paramagnetic solutions. *J. Chem. Phys.*, 27:572–573, 1955.

[6] M. A. Brown and R. C. Semelka. Mr imaging abbreviations, definitions, and descriptions: A review. *Radiology*, 213:647–662, 1999.

[7] Martha D. Bruch. *NMR Spectrosopy Techniques*. Marcel Dekker, Inc., 1996.

[8] E.B. Cady, P. C. D'Souza, J. Penrice, and A. Lorek. The estimation of local brain temperature by in vivo 1h magnetic resonance spectroscopy. *Magn. Reson. Med.*, 33:862–867, 1995.

[9] B.J. Dardzinski and C.H. Sotak. Rapid tissue oxygen tension mapping using 19f inversion-recovery echo-planar imaging of perfluoro-15-crown-5-ether. *Mag. Reson. Med.*, 32:88–97, 1994.

[10] T. L. Davis, K.K. Kwong, R.M. Weisskoff, and B.R. Rosen. Calibrated functional mri: Mapping the dynamics of oxidative metabolism. *Proc. Natl. Acad. Sci.*, 95:1834–1839, 1998.

[11] Andrew E. Derome. *Modern NMR Techniques for Chemistry Research*. Pergamon Press Ltd., 1987.

[12] B.J. D'Othee, G. Rachmuth, J.E. Munasinghe, and E.V. Lang. *Acad. Radiol.*, 10:854–860, 2003.

[13] K. Golman, J.S. Petersson, J.H. Ardenkjaer-Larsen, I. Leunbach, L.G. Wistrand, G. Ehnholm, and K. Liu. Dynamic in vivo oxymetry using overhauser enhanced mr imaging. *J. Magn. Reson. Imaging.*, 12:929–938, 2000.

[14] R. Gruetter, S.A. Weisdorf, V. Rajanayagan, M. Terpstra, H. Merkle, C.L. Truwite, M. Garwood, S.L. Nyberg, and K. Ugurbil. Resolution improvements in in vivo 1h nmr spectra with increased magnetic field strength. *J. Magn. Reson.*, 135:260–264, 1998.

[15] G. Ilangovan, A. Bratasz, H. Li, P. Schmalbrock, J.L. Zweier, and P. Kuppusamy. In vivo measurement and imaging of tumor oxygenation using comebedded paramagnetic particulates. *Magn. Reson. Med.*, 52:650–657, 2004.

[16] M.C. Krishna, S. English, K. Yamada, J. Yoo, R. Murugesan, N. Devasahayam, J.A. Cook, K. Golman, J.H. Ardenkjaer-Larsen, S. Subramanian, and J.B.

Mitchell. Overhauser enhanced magnetic resonance imaging for tumor oxime-
try: coregistration of tumor anatomy and tissue oxygen concentration. *Proc.
Natl. Acad. Sci.*, 99:2216–2221, 2002.

[17] M.I. Lan, N. Beghein, N. Charlier, and B. Gallez. Carbon blacks as epr sensors
for localized measurements of tissue oxygenation. *Magn. Reson. Med.*, 51:1272–
1278, 2004.

[18] D. Li, Y. Wang, and D. J. Waight. Blood oxygen saturation assessment in vivo
using t2* estimation. *Magn. Reson. Med.*, 39:685–690, 1998.

[19] Roger S. Macomber. *A Complete Introduction to Modern NMR Spectroscopy.*
John WileySons, Inc., 1998.

[20] R.P. Mason, S. Hunjan, D. Le, A. Constantinescu, B.R. Barker, and P.S. Wong.
Regional tumor oxyge tension: fluorine echo planar imaging of hexafluorobenzene
reveals heterogeneity of dynamics. *IN. J. Radiat. Oncol.Biol. Phys.*, 42:747–750,
1998.

[21] S. Ogawa, T.M. Lee, A.R. Kay, and D.W. Tank. Brain magnetic resonance
imaging with contrast dependent on blood oxygenation. *Proc. Natl. Acad. Sci.*,
87:9868–72, 1990.

[22] P.E. Parhami and B.M. Fung. *J. Phys. Chem*, 87:1928–1931, 1983.

[23] L. Pauling and C.D. Coryell. The magnetic properties and structure of
hemoglobin, oxyhemoglobin and carbonmonoxyhemoglobin. *Proc. Natl. Acad.
Sci.*, 22:210–216, 1936.

[24] B.K. Siesjo, M. Ingvar, and T. Wieloch. Cellular and molecular events underlying
epileptic brain damage. *Ann N Y Acad Sci.*, 462:207–23, 1986.

[25] B.K. Siesjo and T. Wieloch. Epileptic brain damage: pathophysiology and neu-
rochemical pathology. *Adv. Neurol.*, 44:813–47, 1986.

[26] A.B. Singhal, R.M. Dijkhuizen, B.R. Rosen, and E.H. Lo. Normobaric hyper-oxia reduces mri diffusion abnormalities and infarct size in experimental stroke. *Neurology*, 58:945–52, 2002.

[27] I. Solomon. Relaxation processes in a system of two spins. *Phys. Rev.*, 99:559–565, 1955.

[28] C.S. Springer. *Physichochemical principles influencing magnetopharmaceuticals in NMR in Physiology and Biomedicine*. Academic Press, New York, 1994.

[29] D.R. Tailor, A. Roy, R.R. Regatte, S.R. Charagundla, A.C. McLaughlin, J.S. Leigh, and R. Reddy. Indirect 17o-magnetic resonance imaging of celebral blood flow in the rat. *Magn. Reson. Med.*, 49:479–487, 2003.

[30] K.R. Thulborn, J.C. Waterton, P.M. Matthews, and G. K. Radda. Oxygenation dependence of the transverse relaxation time of water protons in whole blood at high field. *Biochimica et Biophysica Acta*, 714:266–270, 1982.

[31] X.H. Zhu, H. Merkle, J.H. Kwag, K. Ugurbil, and W. Chen. 17o relaxation time and nmr sensitivity of cerebral water and their field dependence. *Magn. Reson. Med.*, 45:543–549, 2001.

[32] X.H. Zhu, Y. Zhang, R.Z. Tian, H.A. Lei, N.A. Zhang, X.L. Zhang, H.E. Merkle, K.A. Ugurbil, and W.E. Chen. Development of (17)o nmr approach for fast imaging of cerebral metabolic rate of oxygen in rat brain at high field. *Proc. Natl. Acad. Sci.*, 99:13194–13199, 2002.

Lisa C. Liu

70 Pacific Street Apt #642B.Cambridge, MA 02139
617-792-1227, lisaliu@mit.edu

Education

2002 – Present **Massachusetts Institute of Technology** Cambridge, MA
- Master of Science in Chemistry, expected June 2005; GPA 4.4/5.0
- Thesis: Tissue Oxymetry Using Magnetic Resonance Spectroscopy

1999 - 2002 **Scripps College** Claremont, CA
- B.A. in Chemistry with Honors, Cum Laude, June 2002; GPA: 11.6/12.0
- Concentration: Mathematics.
  Thesis: Investigation of the rotational barrier in   picolinamide and nicotinamide

Awards

- NSF Honorable Mention award, American Heart Association (AHA) summer research program recipient, Seaver Grant for research program recipient, Accelerated bachelor of art (ABA) degree summer research recipient.
- Goldwater scholarship nominee from Scripps College.

Experience

9/2003 – present **MIT/MGH Nuclear Magnetic Research Center,** Cambridge, MA
Graduate Research Assistant
- Develop a novel and noninvasive in vivo magnetic resonance technique to measure the oxygen content in the brain for master thesis. Integrate engineering principles, clinical medicine, and scientific research, in the field of neuroimaging.
- Skills: animal modeling, ventilation technique, animal surgery for airway, MRI (magnetic resonance imaging), MRS (magnetic resonance spectroscopy), analyzing and simulating spectroscopy data, and statistical package.
- Thesis work will be published in a journal in June.

1/2003 –8/2003 **MIT Francis Bitter Magnetic Laboratory,** Cambridge, MA
Graduate Research Assistant
- Worked on a peptide series as a full-term research assistant.
- Utilized modeling and various solid state NMR spectroscopy technique to determine the structure of this peptide.

9/2002 – 6/2003 **MIT Department of Chemistry** Cambridge, MA
Graduate Teaching Assistant
- Taught thermodynamics and kinetics course for two semesters. Served as a head Teaching Assistant for one semester.
- Responsibilities included giving lectures, leading discussion twice a week for about 30 students, assisting students individually with home work problems, grading problem sets and exams, and updating websites regularly.
- Skills: using Dreamweaver, excellent communication and teaching skills resulted TA of the year and head TA.

9/2000 – 6/2002 **Joint Science Department of Claremont Colleges/UC Riverside** Claremont and Riverside, CA
Undergraduate Research Assistant for thesis in chemistry
- Explored hydrogen bonding in two pyridine derivatives, picolinamide and nicotinamide by using rotational dynamics NMR for senior thesis.
- Skills: NMR, pulse program, data analysis in Mathematica, simulation in Mathematica/Matlab, using Gaussian 98 software for Ab initio calculations.
- Worked on linear prediction and superconductivity project.
- Skills: writing and simulating linear prediction program on Mathematica and working with NMR spectroscopy; writing and designing model for superconductivity by using Matlab.
- Thesis won the honor in Chemistry department and results were published in JACS 2003.

Activities

- Phi Beta Kappa, Sigma Xi Scientific Research Society.
- Tutor for math and organic chemistry; part time job in Dr. Jay Shin's office as an assistant and in Robinsons May as a winter temporary salesperson for perfume department; peer Mentor for Scripps first year; volunteer at Red Cross for Taiwan Earthquake
- Interest: swimming, running, waterpolo, snowboarding, camping, playing piano, politics.

Publications

"The Amide Rotational Barriers in Picolinamide and Nicotinamide: NMR and Ab Initio studies" Ryan A. Olsen, Lisa Liu, Nima Ghaderi, Adam Johns, Mary E. Hatcher, and Leonard J. Mueller. Journal of American Chemical Society, 2003